Available online at www.CivileJournal.org

Civil Engineering Journal

(E-ISSN: 2476-3055; ISSN: 2676-6957)

Vol. 12, No. 06, June, 2026

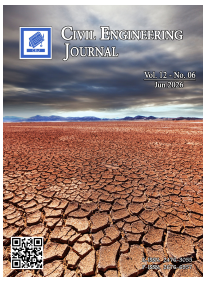

Mechanical Properties and Durability of Variatropic Concrete with Complex Mineral Modifying Additives

Evgenii M. Shcherban' [1], Sergey A. Stel'makh [2], Levon R. Mailyan [2], Diana M. Shakhalieva [3], Andrei Chernil'nik [2], Valery Varavka [4], Alexandr Evtushenko [2], Alexey N. Beskopylny [5*], Yasin O. Özkılıç [2, 6, 7*]

[1] *Department of Engineering Geometry and Computer Graphics, Don State Technical University, Rostov-on-Don 344003, Russia.*

[2] *Department of Unique Buildings and Construction Engineering, Don State Technical University, Rostov-on-Don 344003, Russia.*

[3] *Department of Design, Don State Technical University, Rostov-on-Don 344003, Russia.*

[4] *Research and Education Center "Materials", Don State Technical University, Rostov-on-Don 344003, Russia.*

[5] *Department of Transport Systems, Faculty of Roads and Transport Systems, Don State Technical University, Rostov-on-Don 344003, Russia.*

[6] *Department of Civil Engineering, Faculty of Engineering, Necmettin Erbakan University, Konya 42000, Turkey.*

[7] *Department of Technical Sciences, Western Caspian University, Baku 1001, Azerbaijan.*

Received 09 March 2026; Revised 19 May 2026; Accepted 22 May 2026; Published 01 June 2026

Abstract

In this study, a waste-based complex mineral-modifying additive (CMMA), composed of fly ash (FA), microsilica (MS), and metakaolin (MK) derived from industrial waste, was developed. Concrete specimens were produced using vibration (V), centrifugation (C), and vibro-centrifugation (VC) methods; CMMA was used for replacing cement in amounts ranging from 0% to 20%, with increments of 4%. The compressive strength, water permeability, and freeze-thaw resistance of the resulting concrete were evaluated. The results showed that the optimal CMMA ratio for all production methods was 12%. At this ratio, the compressive strength reached 49.7 MPa, 59.3 MPa, and 63.5 MPa for V, C, and VC concrete mixtures, respectively, corresponding to increases of 10.7%, 15.8%, and 18.7% compared to the control mixture. The same mixtures demonstrated the highest performance in terms of water impermeability, achieving W10, W12, and W14 classifications, respectively. Under freeze-thaw conditions, the lowest strength losses were again observed in the specimens containing 12% CMMA, which were 5.9%, 4.8%, and 3.7%, respectively. Microstructural analyzes have shown that CMMA produces a denser, more homogeneous, lower-porosity cement matrix and reduces microcrack formation. The findings indicate that CMMA is particularly effective when used with centrifugal and vibro-centrifugal production technologies.

Keywords: Variatropic Concrete; Frost Resistance; Compressive Strength; Water Resistance; CMMA; Reinforced Concrete Products.

1. Introduction

As urbanization accelerates and the global economy grows, construction is progressing more rapidly. High construction rates are accompanied by enormous consumption of natural non-renewable resources, including cement, the production of which is accompanied by large CO_2 emissions, and the accumulation of solid demolition waste. All

* Corresponding author: besk-an@yandex.ru; yozkilic@erbakan.edu.tr

https://doi.org/10.28991/CEJ-2026-012-06-021

of this ultimately has a negative impact on the environment [1-3]. This creates a need to identify alternative sources of raw materials for the construction industry, including those suitable for concrete production. Fly ash (FA) is classified as a man-made waste and is used as an active mineral additive, replacing part of the cement in concrete composite technologies [4, 5]. Including 15% FA increases the slump of mixtures and increases the compressive strength of high-strength concrete by 23.2% [6]. Using a mixture of FA and waste glass powder improves the strength and microstructure of concrete [7, 8]. Low-carbon concretes with 20% FA content have better performance properties compared to the control composition [9]. Concrete for 3D printing with a 50% mixture of FA and ground granulated blast furnace slag, introduced instead of part of the cement, demonstrated excellent performance, meeting all printing requirements [10]. FA can be effectively used in the production of reactive powder concrete with a strength of up to 130 MPa [11]. Improvements in the performance properties of concrete with the inclusion of FA are also confirmed by other studies [12-15].

Microsilica (MS) is a man-made waste produced during the gas-cleaning process of industrial electric-arc furnaces. MS has high pozzolanic activity and is used as an active mineral additive for concrete [16]. Waterproof concretes modified with FA and MS have improved frost resistance and fewer capillary pores [17]. Inclusion of an optimal amount of FA and MS mixture in the composition of high-strength concrete allows to increase its water resistance [18]. Reinforced concrete beams in high-chloride environments show decreased corrosion rates when natural pozzolana and MS additives are used [19]. MS in dosages from 6% to 7.5% increases the compressive strength and increases the structural density of specialized solutions designed for the immobilization of radioactive waste concrete [20]. Concrete with rubber crumb used instead of part of the sand, modified with MS, showed improved workability and strength compared to the composition without MS [21]. Including MS helps to reduce the alkali reactivity of fillers used in the production of various types of concrete [22]. Multiple investigations have confirmed that adding MS into composites leads to better physical and mechanical properties [23-26]. Metakaolin, a mineral additive for concrete, is a pozzolanic material created through the thermal activation of aluminosilicate minerals. The properties of concrete can be significantly improved by incorporating MK in an optimal amount [27, 28]. Adding 10% MK to concrete with recycled coarse aggregate enhances its hydration and strengthens its composite properties [29].

Compressive strength of laterite aggregate concrete increased from 35.6 MPa to 53.9 MPa with a 10% MK addition, leading to significant microstructural densification in the transition zones [30]. MK and nanosilica act synergistically, accelerating hydration by approximately 3 hours. This enables the creation of UHPC with strengths reaching 182 MPa [31]. Reinforced concrete beams achieve a 22% boost in compressive strength by incorporating both MK and recycled glass, according to source [32]. With MK concentrations up to 15%, concrete mixes incorporating recycled aggregate can be optimized, leading to the production of curbs with the desired performance characteristics [33]. The addition of MK helps reduce alkali-silicate reactions in reactive coarse aggregate, which ultimately has a beneficial effect on the properties of concrete [34]. MK is considered an environmentally friendly alternative to Portland cement. With an optimal formulation, the use of MK allows for the production of composites with improved properties. The addition of 10% MK and 5% natural zeolite increases the durability of high-strength concrete [35-37]. Eco-friendly concretes with MK and improved strength properties have also been developed in studies by other authors [38-42].

The industrial waste usage such as FA and MS in concrete production is a prospective solution to the environmental improvement. This enables the creation of composites with enhanced characteristics [43-46]. However, FA and MS are waste materials and often exhibit significant differences in their chemical composition. Industrial waste in its original form contains contaminants and pollutions, and has varying moisture content, making its usage impossible without prior preparation. The market offers a wide set of additives, reflecting the significant growth in concrete's additive manufacturing industry [47, 48].

This study proposes developing an organic-mineral additive based on silica-containing components (FA, MS, and MK) and a plasticizing surface-active component. The important role is devoted to assessing its effectiveness of concrete produced by three technologies: vibration (conventional concrete), centrifugation, and vibrocentrifugation (Variatropic concrete). Variatropic concrete is a composite with varying distributions of constituent materials across the cross-section, particularly the coarse aggregate. In centrifuged concrete, the cement-sand mortar and crushed stone are distributed under the influence of centrifugal forces as follows. The outer layer primarily contains large crushed stone grains bonded by mortar; the middle layer contains smaller crushed stone grains and mortar; the inner layer comprises a cement-sand mortar containing the smallest sand fractions and cement particles squeezed out of the outer and middle layers during compaction. A key difference in the structure of vibrocentrifuged concrete compared to centrifuged concrete is the uniform distribution of crushed stone grains within a cement-sand mortar in its outer and middle layers

[46-51]. Developing a new additive from industrial waste for variatropic concrete will broaden its applications and address waste management issues. The scientific novelty of the work lies in the development of a new complex mineral modifying additive (CMMA) based on man-made waste, the creation of new types of concrete manufactured by vibration, centrifugation, and vibrocentrifugation technologies and modified with CMMA, and the determination of the mechanisms of CMMA operation within the composite structure under various manufacturing parameters. The theoretical approach proposed in this paper involves analyzing previously conducted research on similar topics, systematizing previously acquired knowledge, and formulating a core scientific concept. The study utilized standardized methods for assessing the properties of variable-temperature composites, analyzed experimental results, and identified key patterns.

Although many studies have demonstrated that mineral admixtures such as fly ash (FA), microsilica (MS), and metakaolin (MK) improve the mechanical and durability properties of concrete, existing research has largely focused on the effects of these additives on concrete produced using conventional vibration methods. In contrast, the development of CMMA systems and their behavior under different production technologies have not been sufficiently investigated. In particular, limited information is available regarding the performance and distribution mechanisms of such additives in variatropic concretes, whose internal structure is shaped by centrifugal and vibro-centrifugal effects. Furthermore, the combined effects of additive composition, particle distribution, and production technology on concrete performance have not been systematically investigated. Additionally, comprehensive studies that simultaneously examine the effects of multi-component mineral additives on microstructural development and durability properties under different compaction mechanisms are insufficient. Therefore, there is a need for a systematic study that includes the development of a complex mineral-modifying additive and a comprehensive evaluation of its performance under different production technologies. The aim of this study is to create ready-to-use CMMA and to produce vibrated (V), centrifuged (C), and vibrocentrifuged (VC) concretes modified with CMMA, intended for manufacturing reinforced concrete products and structures. The main objectives of this study can be summarized as follows:

- To develop a systematic and reproducible method for producing a complex mineral modifying additive (CMMA) based on industrial waste materials (fly ash, microsilica, and metakaolin), and to characterize its physical, chemical, and morphological properties;
- To design and prepare experimental concrete specimens produced using three different manufacturing technologies—vibration (V), centrifugation (C), and vibrocentrifugation (VC)—incorporating CMMA at varying replacement levels (0–20%) of cement;
- To experimentally evaluate the influence of CMMA content and production technology on the key mechanical and durability properties of concrete, including compressive strength, water resistance, and frost resistance;
- To investigate the microstructural characteristics of the developed concretes using SEM and EDS analyses, with particular emphasis on phase formation, particle distribution, and matrix densification;
- To perform a comparative and quantitative analysis of the experimental results in order to identify the optimum CMMA dosage and to establish relationships between composition, production method, and performance;
- To explain the underlying mechanisms of CMMA action in cementitious systems, including its pozzolanic reactivity, microfilling effect, and its role in promoting the formation of C–S–H and C–A–H phases;
- To assess the combined effect of CMMA and variatropic production technologies (especially centrifugation and vibrocentrifugation) on the structural organization and performance enhancement of concrete;
- To evaluate the practical applicability and engineering feasibility of the developed CMMA-modified concretes for reinforced concrete elements, including their potential use in precast structural components such as pipes, poles, and load-bearing elements;
- To contribute to the development of sustainable construction materials by reducing cement consumption and promoting the utilization of industrial waste in high-performance concrete production.

2. Materials and Methods

2.1. Materials

Raw materials for concrete production, including their types and properties, are detailed in Table 1.

Table 1. Properties of Raw Materials

Indicator	Actual value
Portland cement CEM I 52.5 N (PC) (CEMROS, Stary Oskol, Russia)	
Specific surface area (m^2/kg)	315
Normal density (%)	27
Setting time (min)	160
Setting time (min)	250
Compressive strength at 28 days (MPa)	45.8
Uniform volume change (mm)	0.5
Mineralogical composition of clinker:	
C_3S (%)	67.7
C_2S (%)	12.3
C_3A (%)	8.2
C_4AF (%)	11.8
Quartz sand (QS) (Arkhipovsky quarry, Arkhipovskoye, Russia)	
Bulk density (kg/m^3)	1345
Apparent density (kg/m^3)	2561
The content of dust and clay particles (%)	0.13
Crushed granite, fraction 5-20 mm (CrS) (Granite, Kamennogorsk, Russia)	
Bulk density (kg/m^3)	1455
Apparent density (kg/m^3)	2663
Resistance to fragmentation (wt %)	11.3
The content of lamellar and acicular grains (wt %)	8.5
Fly ash (FA) (Novocherkassk State District Power Plant, Novocherkassk, Russia)	
Bulk density (kg/m^3)	935
SiO_2 (%)	40.92
TiO_2 (%)	0.87
Al_2O_3 (%)	21.9
Fe_2O_3 (%)	9.38
CaO (%)	0.82
MgO (%)	1.68
MnO (%)	0.36
K_2O (%)	5.25
Na_2O (%)	0.9
LOI (%)	17.92
Microsilica (MS) (NLMK, Lipetsk, Russia)	
Bulk density (kg/m^3)	152
SiO_2 (%)	92.1
Al_2O_3 (%)	0.66
Fe_2O_3 (%)	0.85
CaO (%)	1.5
MgO (%)	1.03
Na_2O (%)	0.61
K_2O (%)	1.23
C (%)	0.94
S (%)	0.27
LOI (%)	0.81
Highly active metakaolin VMK-45 GK (MK) (Synergo, Magnitogorsk, Chelyabinsk region)	
Al_2O_3 (%)	42.0
Fe_2O_3 (%)	0.1
SiO_2 (%)	53
Loss on ignition at 1000 °C (%)	1
Bulk density (kg/m^3)	450
Powdered plasticizing additive C-3 (CEMMIX, Moscow, Russia)	
Appearance	Brown powder
pH	8±1

The results of the SEM analysis of FA and MS are presented in Figure 1.

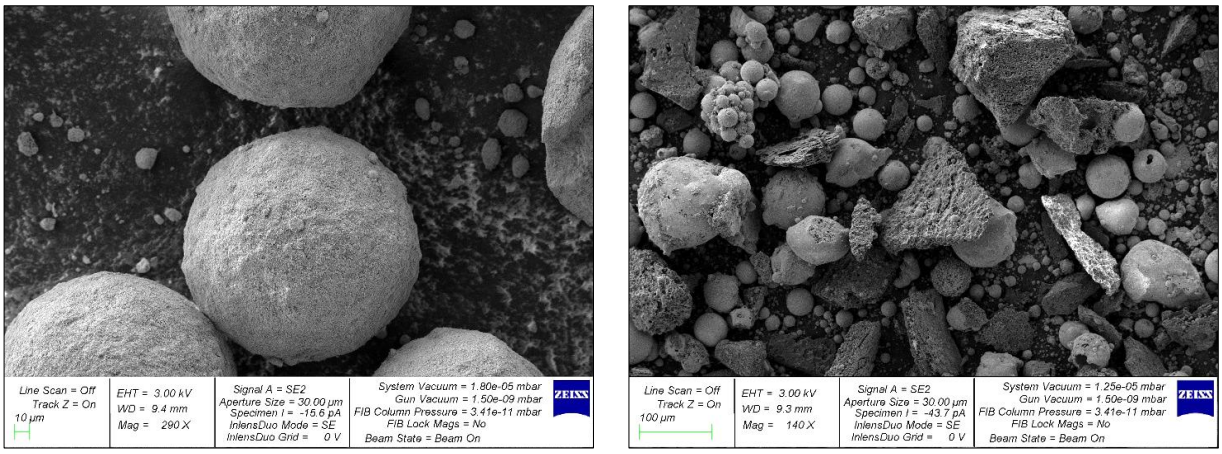

(a) (b)

Figure 1. SEM image:(a) FA at 290× magnification;(b) MS at 140× magnification

FA particles are predominantly spherical. MS consists of agglomerated spherical and irregularly shaped particles. Figure 2 presents the SEM analysis results for MK.

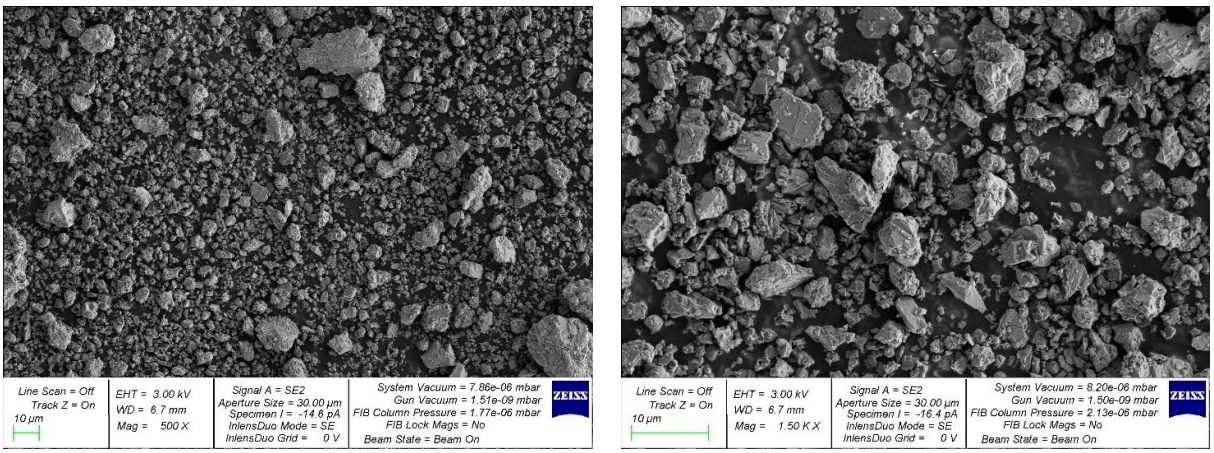

(a) (b)

Figure 2. SEM image of MK:(a) at 500× magnification;(b) at 1500× magnification

MK particles are predominantly plate-shaped and angular. Larger agglomerates of MK particles are observed. Figure 3 illustrates the appearance of the primary components of the raw material

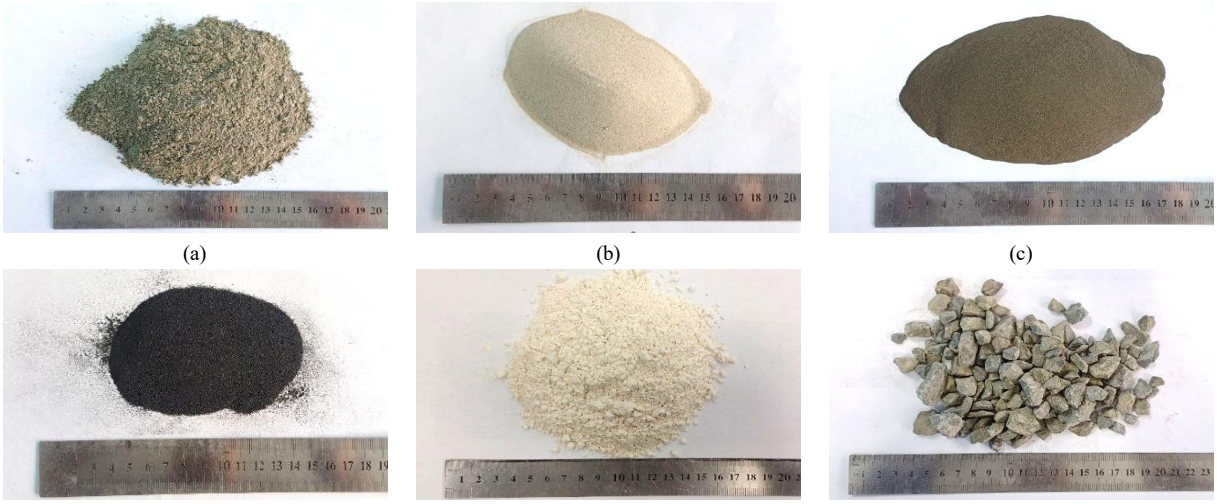

(a) (b) (c)

(d) (e) (f)

Figure 3. Appearance of raw materials:(a) PC; (b) QS; (c) FA; (d) MS; (e) MK; (f) CrS

Figure 4 illustrates the particle size distribution of fine and coarse aggregates.

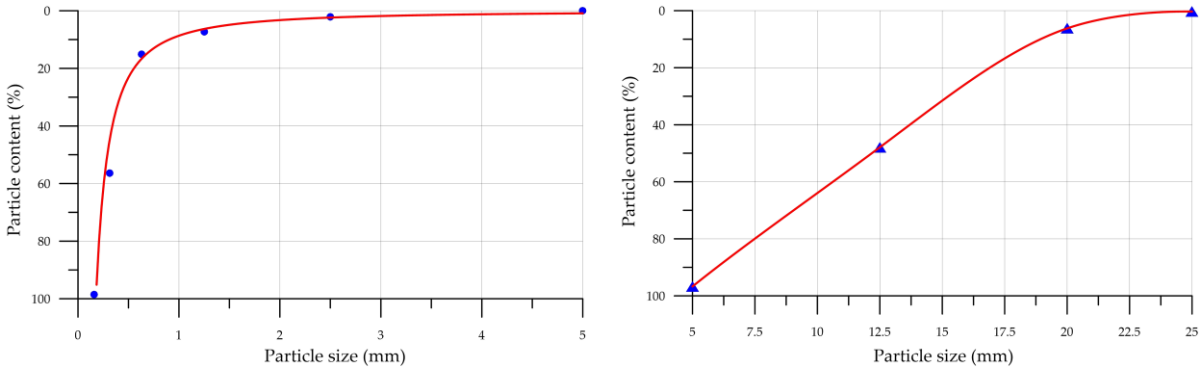

Figure 4. Particle size distribution curves:(a) QS; (b) CrS

A fineness modulus of 1.79 was determined for QS through particle size distribution analysis. The CrS measurement falls within the 5-20 mm range.

Additionally, Figure 5 shows the particle size distribution curves of the finely dispersed mineral components.

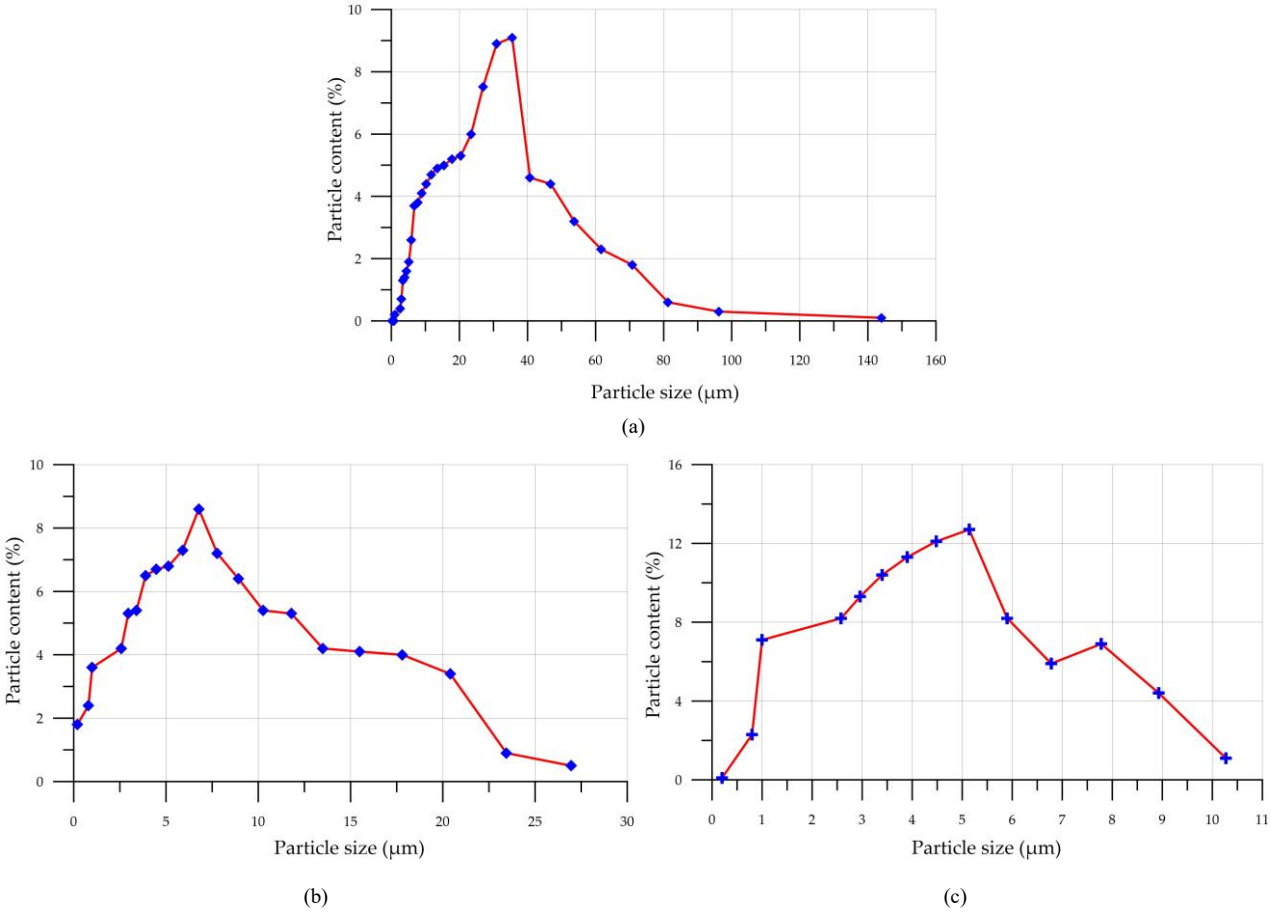

Figure 5. The distribution curves of particle size: (a)FA;(b)MS;(c)MK

Following the particle size analysis results, the fine mineral components have the following distribution:

- FA. The main size range for 79.6% of the particles is 8 to 70 μm, with a maximum frequency of 9.1% at 35.5 μm. The content of particles in the 1 to 8 μm range is 17.6%.
- MS. The main size range, covering 55.9% of the particles, is 5 to 21 μm, with a maximum of 8.6% at 6.78 μm. The particle content in the 0.2 to 5 μm range is 42.7%.
- MK. For 87.6% of the particles, the main size range is 0.2 to 7 μm, with a maximum of 12.7% at 5.14 μm. The proportion of particles in the 7–10.27 μm range is 12.4%.

2.2. Methods

A complex mineral modifying additive (CMMA) was produced from FA, MS, and MK using the following main process steps:

- Purification of FA and MS from contaminants and agglomerated inclusions by sifting through 5 mm and 0.315 mm sieves;
- Drying of FA, MS, and MK in a laboratory drying oven at 50-60 °C to constant weight;
- Dosing of FA, MS, and MK in the quantities required for mixing; mixing of the mineral components and powdered plasticizing additive C-3 in a special container in the following ratio: FA – 70%; MS – 20%; MK – 10%; C-3 – 0.3% of the final weight of the mineral component mixture;
- Loading of CMMA into an Activator-4M planetary ball mill for additional mechanical activation and more uniform distribution of the mineral components. CMMA was mixed for 5 minutes at 600 rpm;
- CMMA was unloaded from the Activator-4M planetary ball mill and packaged in polyethylene bags sealed with a clamp.

The optimal ratio of FA, MS, and MK raw materials for CMMA production was determined during preliminary experimental studies, which assessed the impact of various FA, MS, and MK ratios on the compressive strength of cement matrices. Based on the compressive strength results, the ratio of mineral components that provided the greatest strength gains was selected. Concrete mixes with varying CMMA contents were produced as follows:

- Raw material components were dosed according to the formula presented in Table 2;
- Loading the components into a laboratory concrete mixer in the sequence of PC and CMMA and mixing them dry for 2 minutes; loading QS, CrS, and adding mixing water; mixing all raw materials until a homogeneous consistency was achieved; unloading the concrete mix from the mold and producing experimental samples of variatropic concrete using various technologies.

Table 2. Concrete mix compositions with flow rates per 1 m³

Mixture type	PC (kg/m³)	QS (kg/m³)	CrS (kg/m³)	CMMA (kg/m³)	W (L)
V–0CMMA	420	661	1185	0	180
V–4CMMA	403.2	661	1185	16.8	180
V–8CMMA	386.4	661	1185	33.6	180
V–12CMMA	369.6	661	1185	50.4	180
V–16CMMA	352.8	661	1185	67.2	180
V–20CMMA	336.0	661	1185	84	180
C–0CMMA	420.0	661	1185	0	180
C–4CMMA	403.2	661	1185	16.8	180
C–8CMMA	386.4	661	1185	33.6	180
C–12CMMA	369.6	661	1185	50.4	180
C–16CMMA	352.8	661	1185	67.2	180
C–20CMMA	336.0	661	1185	84	180
VC–0CMMA	420.0	661	1185	0	180
VC–4CMMA	403.2	661	1185	16.8	180
VC–8CMMA	386.4	661	1185	33.6	180
VC–12CMMA	369.6	661	1185	50.4	180
VC–16CMMA	352.8	661	1185	67.2	180
VC–20CMMA	336.0	661	1185	84	180

Before producing experimental samples of V, C, and VC concrete, the slump of fresh concrete was determined with varying doses of CMMA added in place of part of the binder. The slump of fresh concrete varied from 2 to 9 cm. With increasing CMMA content, slump values decreased within acceptable limits. The presence of the C-3 plasticizing additive in the CMMA reduced the water demand of the mineral components.

Vibrated concrete specimens were prepared by pouring the mix into metal molds and vibrating them on a lab table for a minute. Compaction was followed by smoothing of the sample surfaces. Samples were centrifuged in the following sequence. The concrete mixture was spun at 50-100 rpm in a metal mold for 5 minutes. Afterward, the concrete mix

underwent a 10-minute period of intensive compaction at speeds of up to 600 rpm. After compaction, the sludge was drained from the mold. The entire centrifugation cycle took 20 minutes. Vibro- centrifugation was conducted under the same parameters as standard centrifugation, except that specialized clamps with protrusions 5 mm high, 20 mm long, and spaced at 30 mm intervals were placed on the unit's shafts to induce vibration. Following production, the V, C, and VC concrete experimental specimens were cured for one day before being extracted from their molds. The specimens were then cured for another 27 days under conditions of 20 ± 2 ℃ and 60 ± 10% relative humidity. Following the procedure in Beskopylny et al. [52], cubes of 100×100×100 mm and 150×150×150 mm were sawn from the C and VC concretes on a stone-cutting machine at 28 days.

Figure 6 illustrates the experimental design for V, C, and VC concretes modified with CMMA.

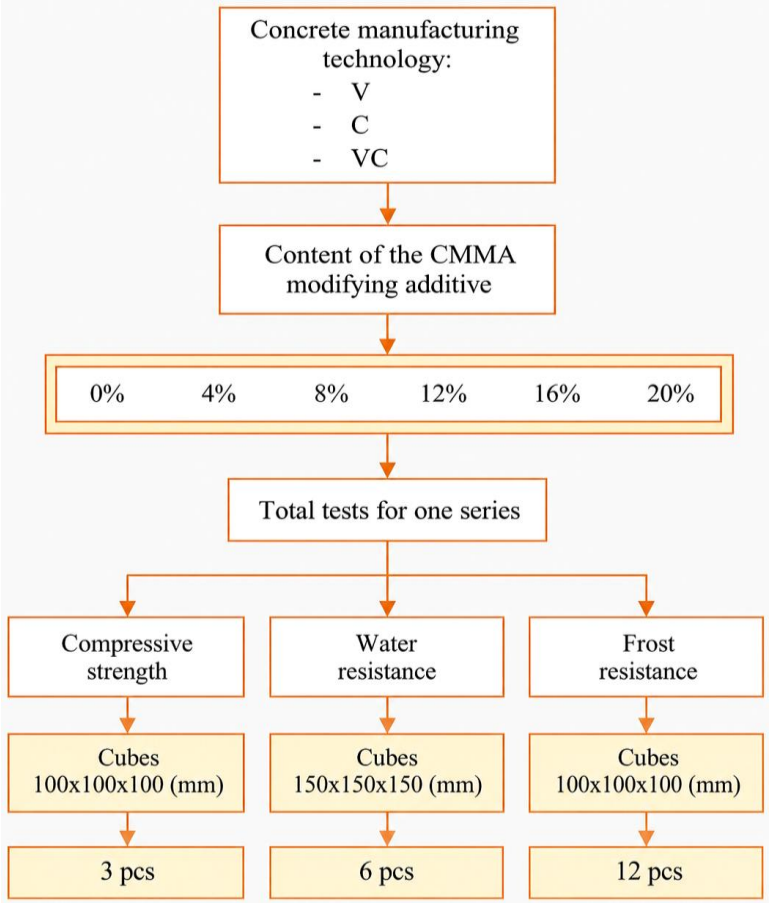

Figure 6. Experimental design

Standard methodologies [53-56] were employed to determine the compressive strength (R, MPa) of V, C, and VC concrete. Each specimen underwent testing at 28 days of age. The concrete samples underwent testing and were subjected to increasing load until they broke, with the loading rate maintained at (0.6 ± 0.2) MPa/s. With a precision of 0.1 MPa, Equation 1 was used to determine the compressive strength. The arithmetic mean of the two strongest specimens in each group of three was used to determine the compressive strength.

$$R = \alpha \frac{F}{A} \quad (1)$$

where F is the ultimate load (N); A is the cross-sectional area of the specimen(mm2); and α is a coefficient accounting for specimen dimensions (for specimens with a side length of 100 mm, α = 0.95).

The water resistance of concrete was determined using a rapid method using the AGAMA-2RM instrument (RusPribor, Russia) under the requirements of GOST 12730.5-2018 [57]. Before testing, the specimen's surface was cleaned. A special 8-mm-diameter sealing mastic rope was then prepared and placed on the chamber flange in a groove along its midline. The chamber flange was then positioned on the prepared section of the specimen and pressed firmly against its surface, after which the measurement process began. Based on the measurement results, the instrument's display showed the concrete's air penetration resistance (m_c, s/cm³) and the corresponding water resistance grade (W).

According to method of GGOST 10060-2012 [58], the frost resistance (F, cycles) of V, C, and VC concrete was established. Table 3 provides the conditions for using the accelerated method to assess the frost resistance of concrete.

Table 3. Test conditions for determining frost resistance

Sample type and quantity	Duration, h		
	Saturation medium: 5% aqueous NaCl solution	Freezing medium and temperature: 5% aqueous NaCl solution, minus (50±2)°C	Medium and thawing temperature: 5% aqueous NaCl solution, (20±2)°C
Control samples – 6 pcs.	48	–	–
Main samples – 6 pcs.	48	7	3.5

The saturated control specimens were then removed, cleaned, weighed, and assessed for strength. Formula 1 was used to determine the compressive strength of each control specimen. Following repeated freeze-thaw cycles, the principal specimens were inspected, brushed, wiped with a damp cloth, weighed, and assessed for strength. The frost resistance findings were handled as outlined in GGOST 10060-2012 [58]. The specimens were considered having passed the frost resistance test if the ratio $X^{ll}_{\min} \geq 0.9\, X^{l}_{\min}$ was observed, the mass loss did not exceed 2%, and the specimens were free of cracks, chips, or flaking of ribs (X^{ll}_{min} is the lower limit of the confidence interval for the main specimens after freezing and thawing the specimens; X^{l}_{min} is the lower limit of the confidence interval for the control specimens).

The morphology of FA, MS, MK, CMMA, and Variatropic concrete particles modified with CMMA was assessed using a ZEISS CrossBeam 340 scanning electron microscope (Carl Zeiss Microscopy GmbH, Jena, Germany) equipped with an Oxford Instruments X-Max 80 X-ray microanalyzer.

3. Results and Discussion

3.1. Results of CMMA Property Evaluation

The results of SEM and EDS analyses of CMMA are presented in Figures 7 and 8, respectively.

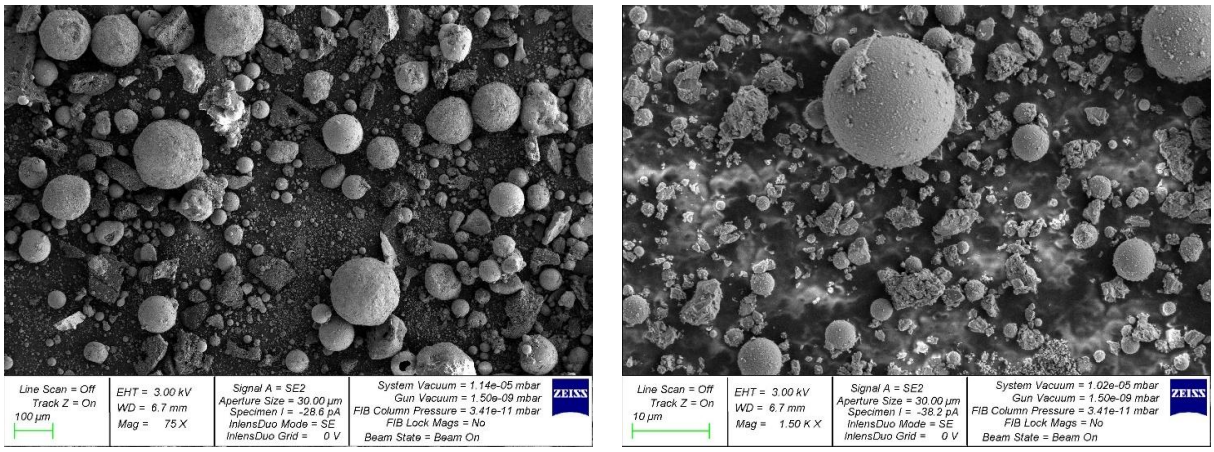

(a) (b)

Figure 7. SEM image of CMMA:(a) at 75× magnification;(b) at 1500× magnification

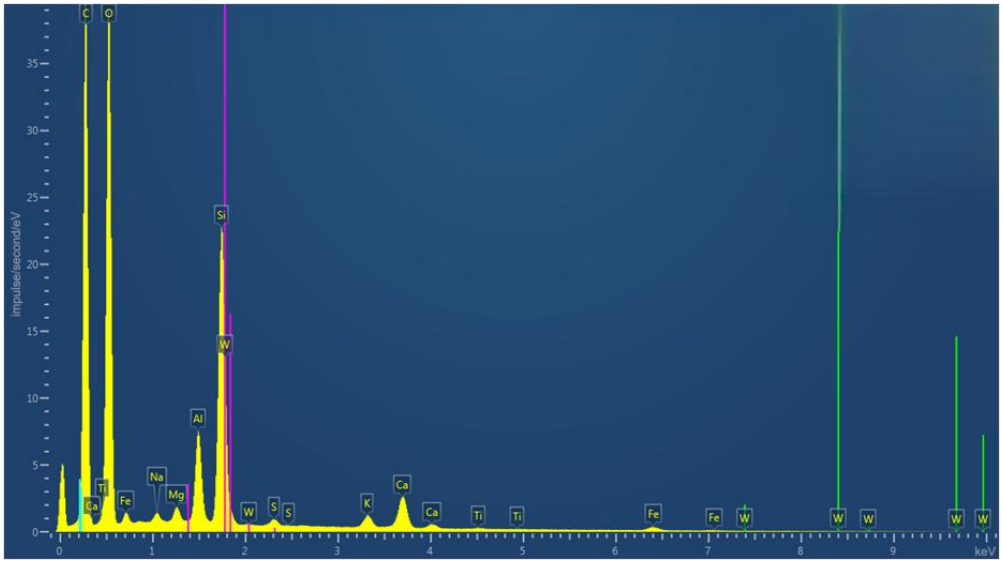

Figure 8. EDS CMMA

The complex mineral- modifying additive is a mixture of the mineral components fly ash, microsilica, and metakaolin, each with different particle size distributions. MS and MK particles are uniformly distributed among the FA particles. No agglomerated clusters are observed.

According to the EDS analysis, the elemental composition of CMMA comprises the following elements: C; O; Si; Ca; Al; Fe; K; Mg; Na; S; Ti.

3.2. Results of Assessing the Properties of V, C, and VC Concretes Modified with CMMA

The findings in Figure 9 detail the compressive strength evaluations for vibrated (V), centrifuged (C), and vibrocentrifuged (VC) concrete specimens with varying CMMA additive amounts.

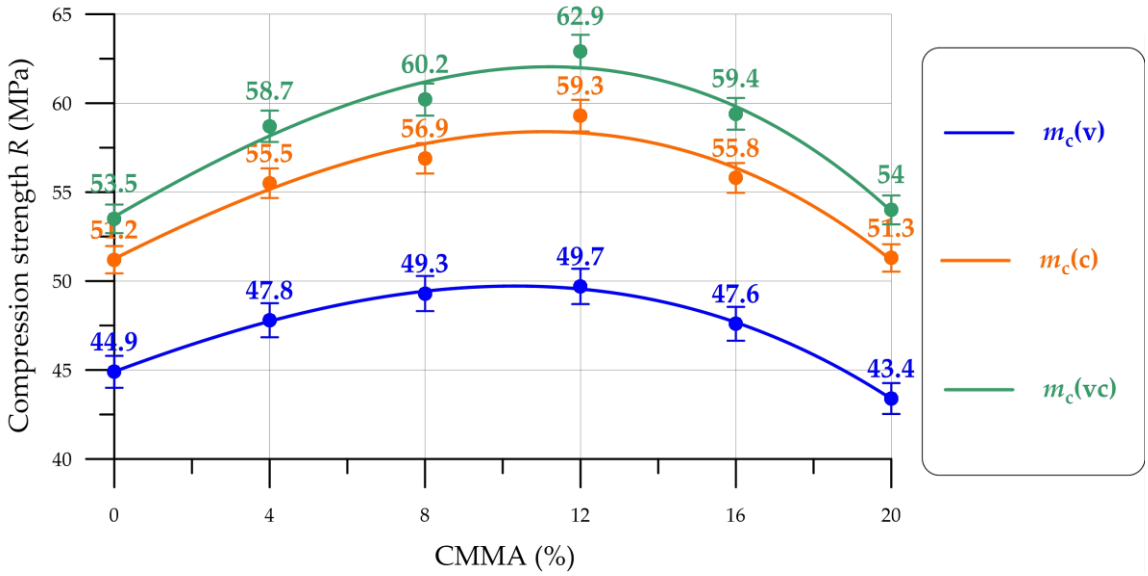

Figure 9. Compressive strength of V, C, and VC concretes versus CMMA content

The compressive strength analysis in Figure 9 shows that V, C, and VC concretes with up to 16% CMMA replacing cement exhibited increased strength. The compressive strength was highest at 12% CMMA content. Among the vibrated concretes, the V–12CMMA composition has the highest compressive strength, 49.7 MPa, which is 10.7% higher than the control. Among the centrifuged and vibrocentrifuged concretes, the C–12CMMA and VC–12CMMA compositions have maximum compressive strengths of 59.3 MPa and 63.5 MPa, which are 15.8% and 18.7% higher than the control value. V, C, and VC concretes modified with 16% CMMA exhibit compressive strengths that are 6%–11% higher than the control values. However, at 20% CMMA, the strength of the Variatropic composites decreases to values comparable to those of the control compositions. The sharp decrease in compressive strength at 20% CMMA indicates that incorporating more than 20% of this additive in V, C, and VC concretes, replacing a portion of the cement, is impractical and will cause a greater reduction in strength. This improvement in compressive strength can be attributed to the combined pozzolanic and microfilling effects of CMMA. The fine particles of microsilica and metakaolin fill the voids between cement grains, leading to denser particle packing and reduced porosity. Simultaneously, the pozzolanic reaction of FA, MS, and MK with calcium hydroxide promotes the formation of additional C–S–H and C–A–H gels, which enhance the bonding within the cement matrix. However, at higher replacement levels (e.g., 20%), the dilution effect predominates because of insufficient cement content, resulting in reduced strength. The values of the coefficients of determination of the experimental dependencies of the compressive strength V, C and VC concrete modified with different dosages of CMMA were: $R_v^2 = 0.9659$; $R_c^2 = 9597$; $R_{vc}^2 = 0.9984$. Table 4 illustrates the effect of varying CMMA quantities on the compressive strength (ΔR) of V, C, and VC concretes.

Table 4. Changes in Compressive Strength of V, C, and VC Concretes Depending on CMMA Content

ΔR (%)	CMMA content (%)				
	4	8	12	16	20
ΔR_v (%)	6.5	9.8	10.7	6.0	–3.3
ΔR_c (%)	8.4	11.1	15.8	9.0	0.2
ΔR_{vc} (%)	9.7	12.5	17.6	11.0	0.9

Table 4 shows that the CMMA modification is most effective when combined with vibro-centrifugal compaction technology.

Figure 10 further shows rapid tests for water-resistance grade.

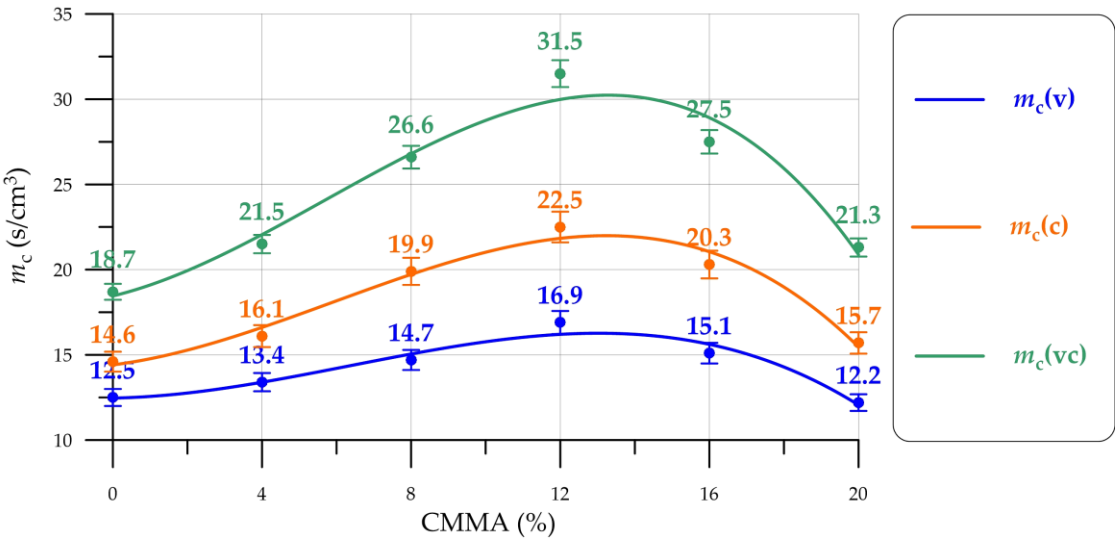

Figure 10. Air penetration resistance of concrete V, C, and VC as a function of CMMA content

The air-penetration resistance values (Figure 10) for concretes V, C, and VC tend to increase as CMMA modification levels rise from 4% to 12%. Concretes V, C, and VC exhibit their maximum air-penetration resistance values when using 12% CMMA. The air penetration resistance values of vibrated concrete for V–0CMMA and V–4CMMA compositions were 12.5 s/cm^3 and 13.4 s/cm^3, respectively, which, according to the requirements of EN 12390-2:2019 [54], corresponds to the W8 grade, where m_c values range from 9.5 to 13.7 s/cm^3. Vibrated concrete of compositions types V–8CMMA, V–12CMMA and V–16CMMA have concrete air penetration resistance values equal to 14.7 s/cm^3, 16.9 s/cm^3 and 15.1 s/cm^3, which, according to the requirements of GOST 12730.5-2018 [57], corresponds to the W10 grade, where the m_c values vary from 13.8 to 19.6 s/cm^3. Concrete composition V with the maximum content of the V–20CMMA additive has the W8 water-resistance grade. Centrifuged concrete of compositions types C–0CMMA and C–4CMMA have concrete air penetration resistance values of 14.6 s/cm^3 and 16.1 s/cm^3, which corresponds to the W8 water resistance grade. The values of concrete resistance to air penetration for compositions C–8CMMA, C–12CMMA and C–16CMMA were 19.9 s/cm^3, 22.5 s/cm^3 and 20.3 s/cm^3, which, according to the requirements of GOST 12730.5-2018 [57], corresponds to the W12 grade, where the m_c values vary from 19.7 to 29.0 s/cm^3.

Concrete composition C with the maximum content of the C–20CMMA additive has a water-resistance grade of W10. Vibro-centrifuged concrete of the control composition VC–0CMMA has a water resistance grade of W10. Compositions of the VC–4CMMA and VC–8CMMA types have a water resistance grade of W12. The VC–12CMMA concrete composition has an air penetration resistance value of 31.5 s/cm^3, which, according to the requirements of GOST 12730.5-2018 [57], corresponds to the W14 grade, where m_c values range from 29.1 to 42.0 s/cm^3. The VC–16CMMA and VC–20CMMA compositions have a water resistance grade of W12. Primarily, the pore structure becomes more refined, leading to increased water resistance upon CMMA incorporation. The microfilling effect of fine particles reduces capillary pore connectivity, while the formation of additional hydration products further blocks fluid transport pathways. As a result, the permeability of the concrete decreases significantly, especially at the optimum CMMA content. The superior performance of VC concretes can be attributed to a more uniform distribution of fine particles, which enhances pore discontinuity and reduces permeability. The values of the coefficients of determination of the experimental dependencies for determining the water resistance V, C and VC concrete modified with different dosages of CMMA were $R_v^2 = 0.9577$; $R_c^2 = 9718$; $R_{vc}^2 = 0.9434$.

Table 5 shows the changes in air penetration resistance (Δm_c) of V, C, and VC concretes containing different amounts of CMMA.

Table 5. Changes in air penetration resistance of V, C, and VC concretes depending on CMMA content

Δm_c (%)	CMMA content (%)				
	4	8	12	16	20
$\Delta m_{c(v)}$ (%)	7.2	17.6	35.2	20.8	–2.4
$\Delta m_{c(c)}$ (%)	10.3	36.3	54.1	39.0	7.5
$\Delta m_{c(vc)}$ (%)	15.0	42.2	68.4	47.1	13.9

The graphs in Figure 11 display the changes in compressive strength for V, C, and VC concrete samples (both control and main) containing different CMMA levels, following a set amount of freezing and thawing.

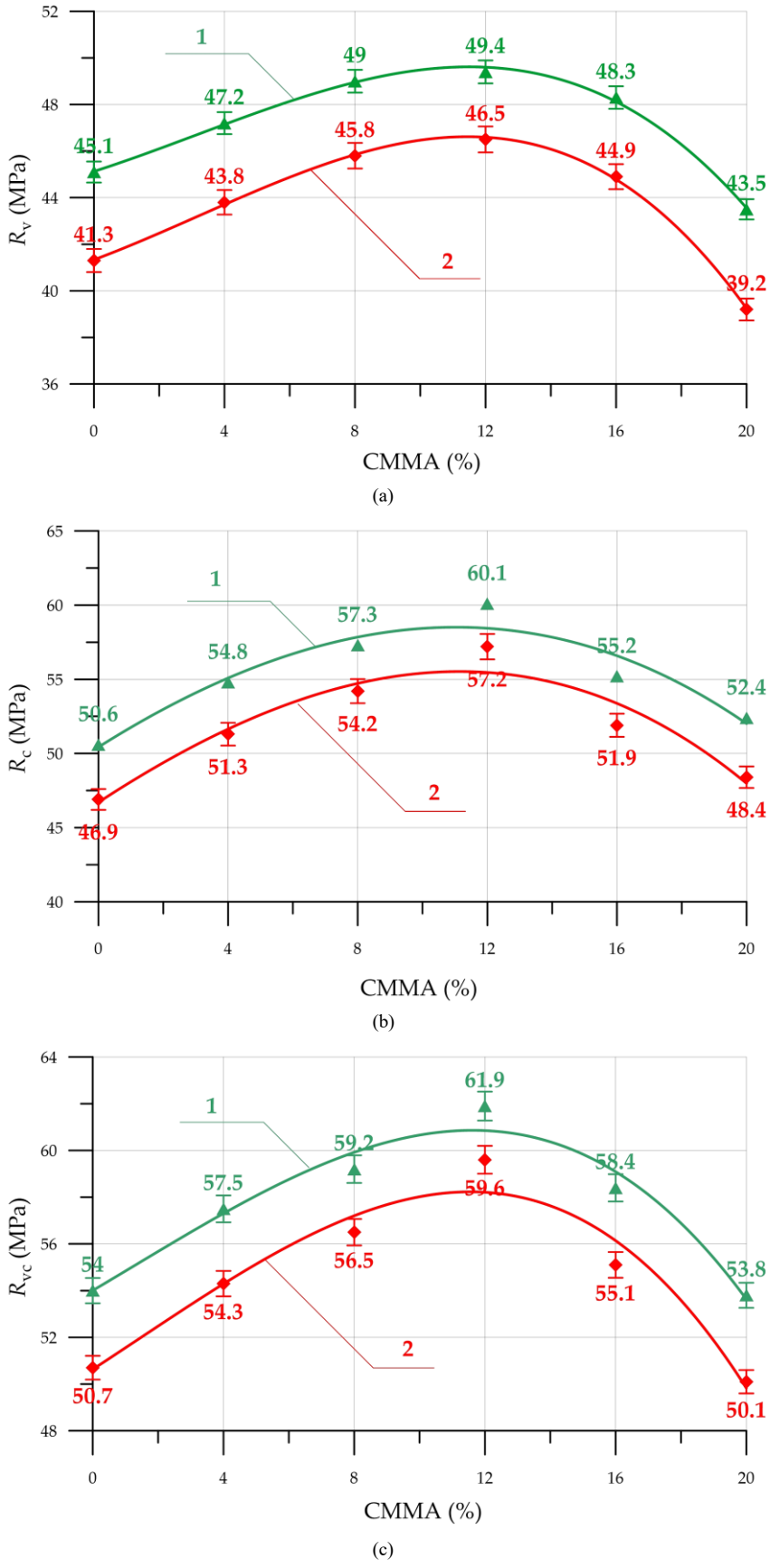

Figure 11. Compressive strength of control (1) and base (2) concrete specimens with different CMMA contents after a given number of freeze-thaw cycles:(a) V, 2 – after 7 cycles;(b) C, 2 – after 9 cycles;(c) VC, 2 – after 11 cycles (1– green, 2– red)

Varying amounts of CMMA resulted in different compressive strengths in the concrete, as shown below. The base specimens with the V–12CMMA composition exhibited the lowest compressive strength loss of 5.9%. The base specimens, comprising the control composition V and those containing 4%, 8%, 16%, and 20% CMMA exhibited higher percentage losses of strength, ranging from 6.5% to 9.9%. The mass losses after 7 freeze-thaw cycles for V–0CMMA, V–4CMMA, V–8CMMA, V–12CMMA, V–16CMMA, and V–20CMMA concretes were 1.7%, 1.6%, 1.5%, 1.4%, 1.6%, and 1.8%, respectively. The mass loss values for all V-grade concrete compositions did not exceed 2%, and the condition (Table 6) was $X^{II}_{\min} \geq 0.9\,X^{I}_{\min}$ met. Consequently, the V-grade concrete specimens passed the frost resistance test, achieving a frost resistance grade of F200. According to the requirements of the test method [58], the frost resistance grade F200 is assigned if the main concrete specimens withstand 5 to 7 freeze-thaw cycles, they are free of defects, the ratio $X^{II}_{\min} \geq 0.9\,X^{I}_{\min}$ is observed and the mass loss does not exceed 2%.

For C concrete, the C–12CMMA composition exhibited the lowest loss of strength among the main specimens, amounting to 4.8%. C concrete compositions, in which the CMMA content was 0%, 4%, 8%, 16%, and 20%, exhibited strength losses in the main specimens ranging from 5.4% to 7.6% after 9 freeze-thaw cycles. The mass losses after 9 freeze-thaw cycles for compositions of Type C–0CMMA, C–4CMMA, C–8CMMA, C–12CMMA, C–16CMMA, and C–20CMMA were 1.6%, 1.4%, 1.2%, 1.1%, 1.3%, and 1.4%, respectively. According to the test results, the C concretes demonstrated mass losses not exceeding 2%, meeting the condition for all compositions $X^{II}_{\min} \geq 0.9\,X^{I}_{\min}$ (Table 6). Therefore, the C samples passed the frost-resistance test, achieving an F300 grade. The test methodology [58] stipulated that a frost resistance grade of F300 would be given if the primary concrete samples endured 8-11 freeze-thaw cycles while maintaining a specific ratio $X^{II}_{\min} \geq 0.9\,X^{I}_{\min}$ and experiencing a mass loss of 2% or less. Among the VC concretes, the VC–12CMMA composition exhibited the lowest compressive-strength loss (3.7%) after 11 freeze-thaw cycles. For all other VC concrete compositions, the strength reductions ranged from 4.6% to 6.9%. The mass loss after 11 freeze-thaw cycles for the VC–0CMMA, VC–4CMMA, VC–8CMMA, VC–12CMMA, VC–16CMMA, and VC–20CMMA concrete mixes was 1.4%, 1.3%, 1.0%, 0.7%, 1.1%, and 1.2%, respectively. According to the test results, the VC concretes exhibited mass losses that did not exceed 2%, and $X^{II}_{\min} \geq 0.9\,X^{I}_{\min}$ this condition was met for all compositions (Table 6). Consequently, the VC concrete specimens achieved an F300 frost resistance rating, showing that they passed the test.

Table 6. Frost resistance calculation for Variatropic concretes with CMMA

Mixture type	Δm (%)	$X^{II}_{min} \geq 0,9X^{I}_{min}$
V–0CMMA	1.7	39.9≥39.6
V–4CMMA	1.6	42.7≥40.4
V–8CMMA	1.5	43.3≥42.2
V–12CMMA	1.4	44.4≥42.8
V–16CMMA	1.6	42.3≥40.3
V–20CMMA	1.8	38.2≥37.9
C–0CMMA	1.6	45.5≥43.4
C–4CMMA	1.4	48.7≥47.8
C–8CMMA	1.2	51.5≥50.0
C–12CMMA	1.1	54.1≥51.3
C–16CMMA	1.3	50.4≥48.6
C–20CMMA	1.4	45.5≥45.3
VC–0CMMA	1.4	48.6≥47.2
VC–4CMMA	1.3	52.9≥49.6
VC–8CMMA	1.0	54.9≥51.4
VC–12CMMA	0.7	56.8≥53.9
VC–16CMMA	1.1	52.7≥ 51.0
VC–20CMMA	1.2	47.1≥46.8

The improved frost resistance of CMMA-modified concretes can be associated with the reduction in pore size and pore connectivity. A denser matrix limits water ingress and reduces the internal stresses generated during freezing. Additionally, the presence of fine particles may contribute to the formation of a more stable pore structure, thereby mitigating damage caused by cyclic freezing and thawing. The lower strength losses observed in VC concretes further confirm the beneficial effect of improved particle distribution and matrix integrity.

The values of the coefficients of determination of the experimental dependencies for determining the frost resistance V, C and VC concrete modified with different dosages of CMMA were: $R_v^2 = 0.9991$; $R_c^2 = 9178$; $R_{vc}^2 = 0.9440$. It is important to note that this study utilized an accelerated methodology for determining the frost resistance grades V, C, and VC concrete within a short timeframe. This methodology allows for a rapid assessment of the impact of adopted formulation and process solutions on the frost resistance of concrete. For assessing the frost resistance of composites planned for use in specific climate regions, it is best to use traditional methods, which utilize laboratory-reproducible temperature regimes that most closely approximate actual operating conditions.

Thus, based on the experimental studies of V, C, and VC concretes with CMMA, the following conclusions can be drawn:

- *Compressive Strength:* CMMA modification of V, C, and VC concretes at 12% provides the largest increases in compressive strength, amounting to 10.7%, 15.8%, and 17.6%, respectively.
- *Water Resistance:* The water resistance grade increases. The best results were recorded with 12% CMMA. For V concrete, the water-resistance grade increased from W8 to W10. For C concrete, the water-resistance grade increased from W10 to W12. For VC concrete, the water resistance grade increased from W10 to W14.
- *Frost Resistance:* The resistance of V, C, and VC concretes to exposure to alternating freeze-thaw cycles increases. The lowest losses in compressive strength of the base specimens after a given number of freeze-thaw cycles were recorded for V, C, and VC concretes modified with 12% CMMA.

The existence of an optimum CMMA content (12%) can be explained by the balance between beneficial pozzolanic and microfilling effects and the adverse dilution effect. At lower replacement levels, the additional hydration products and improved packing density dominate, enhancing strength and durability. Beyond the optimum level, the reduction in cement content limits the formation of primary hydration products, leading to a decline in mechanical performance.

3.3. Interpretation of the Mechanism of CMMA Action in the Cement Matrix Structure

CMMA admixture consists of finely dispersed mineral components FA, MS, and MK, which have been further activated by mechanical milling with a powdered plasticizing additive. CMMA is a highly active pozzolan that effectively undergoes hydration reactions and actively reacts with free $Ca(OH)_2$. CMMA particles initiate the crystallization of calcium silicate hydroxides (CSH) and calcium aluminate hydroxides (CAH) during cement hardening's initial phase [59, 60]. The presence of oxide systems SiO_2, Al_2O_3, Fe_2O_3, and CaO, which are contained in various types of mineral components (FA, MS, and MK) and exhibit increased synergy, allows for the formation of low-basicity calcium silicate hydroxides and aluminosilicate hydroxides through direct interaction with Portland cement particles. Additional CSH and CAH formation leads to changes in the morphology of newly formed cement systems. A denser, more homogeneous cement matrix with fewer capillary pores is achieved through the formation of a significant number of new crystalline intergrowths [61]. A graphical illustration of the mechanism of CMMA action in the cement matrix is presented in Figure 12. These effects make it possible to obtain V, C, and VC concretes with improved compressive strength, water resistance, and frost resistance.

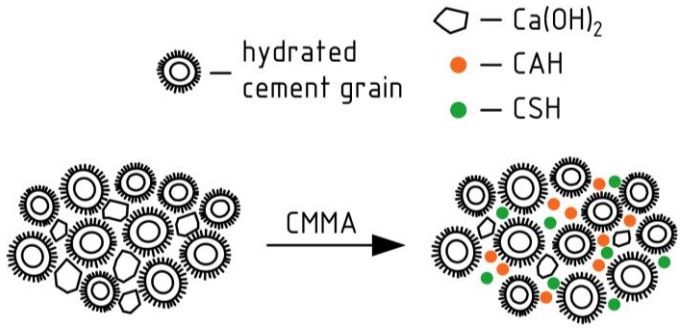

Figure 12. Graphic illustration of the mechanism of CMMA action in the cement matrix structure

Compared with V concretes, C and VC concretes containing 12% CMMA exhibit larger increases in compressive strength. The greater effectiveness of CMMA in C and VC concretes can be attributed to the centrifugal and vibro-centrifugal compaction mechanisms. During compaction, centrifugal forces act on all raw components of the concrete mix, including CMMA particles. Under the influence of centrifugal forces, CMMA particles migrate longitudinally through the entire thickness of the formed annular cross-sectional element, including the filtration channels. The addition of vibrations allows CMMA particles to migrate transversely as well. When evenly distributed within the cement matrix, CMMA promotes the formation of CSH and CAH gels, leading to a stronger structure. Smaller CMMA particles are also embedded between cement grains, increasing the grain packing density in the cement matrix [62-65]. Furthermore, the number of capillary pores and structural defects (microcracks, voids, etc.) is reduced. The targeted action of centrifugal forces, combined with vibration, allows CMMA particles to be distributed more uniformly throughout the composite structure, thereby enhancing CMMA's overall modifying effect.

The optimal CMMA dosage for concrete produced using three different technologies (V, C, and VC) is 12%, demonstrating the versatility of this indicator across various casting technologies. However, if the concrete formulation changes, such as the cement grade, the type of coarse and fine aggregate, their ratios, and the water-cement ratio, the optimal CMMA dosage will change.

3.4. Results of SEM and EDS Analysis of the Structure of V, C, and VC Concretes Modified with CMMA

The microstructural features of C and VC concretes modified with 12% CMMA were assessed using specimens of V–12CMMA, C–12CMMA, and VC–12CMMA. Microstructural study findings are shown in Figures 13 to 15.

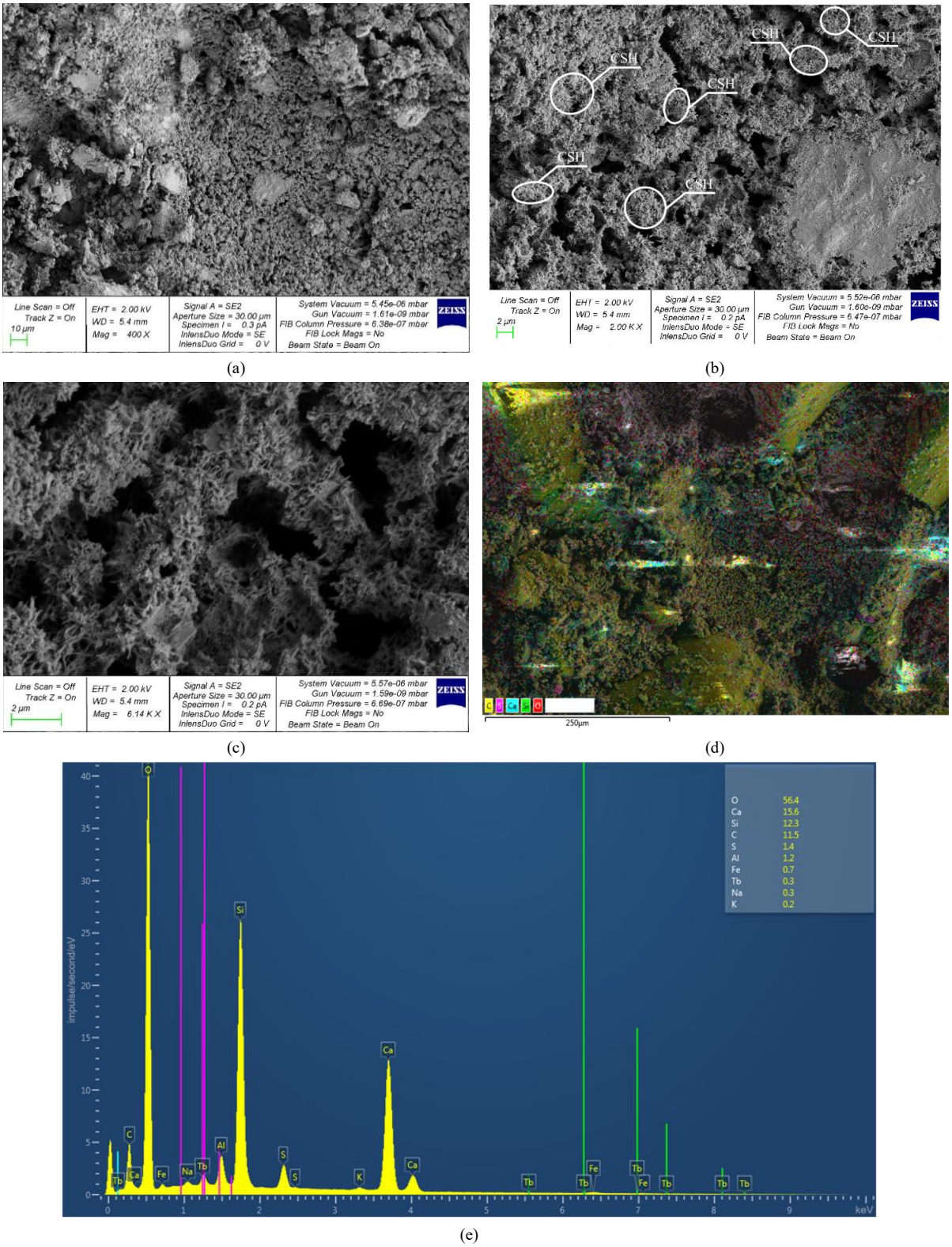

(a) (b) (c) (d) (e)

Figure 13. V–12CMMA structure: (a) 400×; (b) 2000×; (c) 6140×; (d) multilayer EDS map; (e) EDS

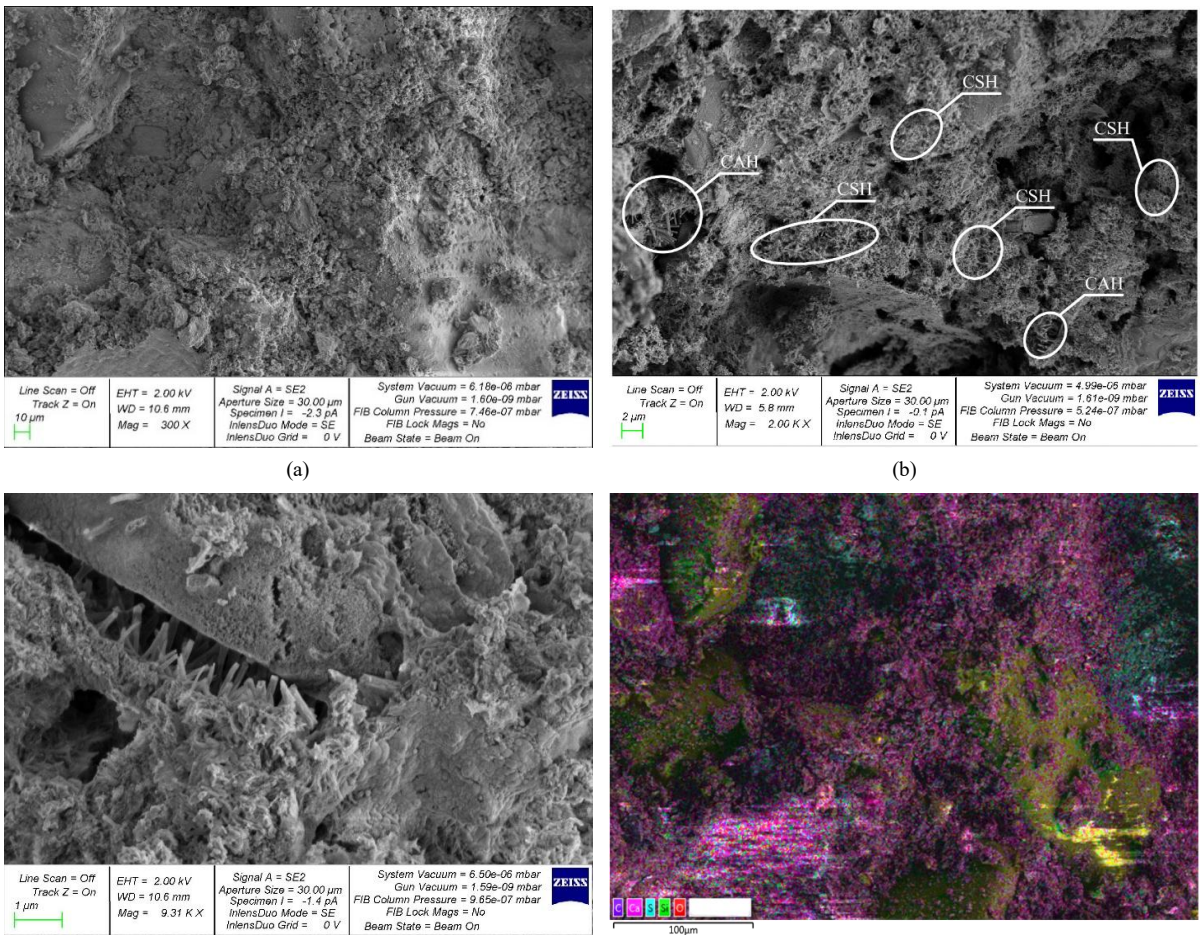

Figure 14. C–12CMMA structure: (a) 300×; (b) 4000×; (c) 9310×(d) multilayer EDS map; (e) EDS

The microstructure of a vibrated concrete sample, altered with CMMA, is depicted in Figure 13. The vibrated concrete modified with CMMA has a homogeneous cement matrix structure, which is largely due to the high pozzolanic activity of the additive. Multiple clusters of C-S-H zones are observed. Energy-dispersive X-ray spectroscopy data showed that the use of CMMA promotes the formation of strong and stable low-basic calcium hydrosilicates C-S-H(I) with a Ca/Si ratio of 1.3. Photographs illustrating the microstructure of centrifuged concrete that has been modified with CMMA are displayed in Figure 14.

Centrifuged concrete containing CMMA also has a homogeneous, well-organized cement matrix structure. Various clusters of CSH and CAH have been noted. Energy-dispersive X-ray spectroscopy results show a Ca/Si ratio of 1.1,

confirming the formation of strong, stable low-basicity calcium silicate hydroxides, CSH(I), resulting from CMMA modification. Figure 15 shows images illustrating the microstructure of vibrocentrifuged concrete modified with CMMA.

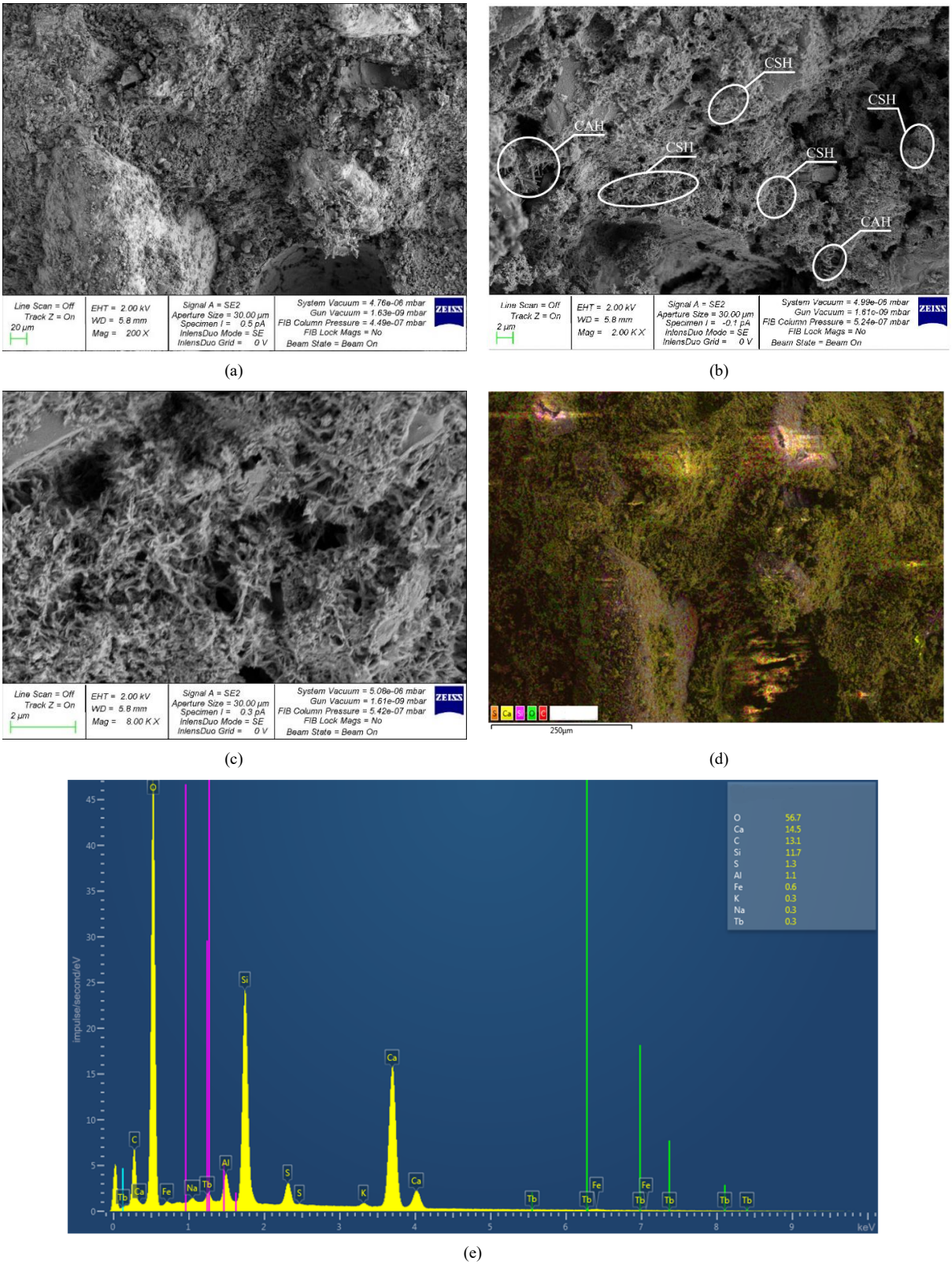

Figure 15. VC–12CMMA structure: (a) 200×;(b) 2000×; (c) 8000×; (d) multilayer EDS map; (e) EDS

The cement matrix of the vibrocentrifuged composites exhibits a homogeneous, organized structure containing multiple clusters of CSH and CAH. A Ca/Si ratio of 1.2 indicates the presence of low-basicity calcium silicate hydroxides (CSH(I)), formed due to CMMA modification.

Microstructural and energy-dispersive analysis of V, C, and VC concretes modified with the optimal amount of CMMA confirms the effectiveness of this additive. Due to the pozzolanic activity of CMMA, a denser and more uniform cement matrix structure is formed early in the composite's curing process. The pozzolanic components act as additional crystallization sites, actively interacting with free $Ca(OH)_2$ to form additional CSH and CAH. The basicity of CSH gels also decreases, confirming the effective interaction of CMMA with cement hydration products. The matrix gains strength and durability due to a reduction in micropores.

3.5. Discussion

A novel mineral admixture, derived from industrial waste, was developed in this research. Incorporating it into concrete as a partial replacement for cement leads to increased composite strength and improved durability. The study's findings align with and are validated by previous research (see Table 7).

Table 7. Effect of mineral admixtures on the properties of cement composites

Source	Additive	Modification parameter	Result
Ali et al. [62]	MK / MS	5%/10%	Compressive strength increases of 17%-23%. Concrete production costs reduced.
Malaiškienė & Jakubovskis [63]	MK + MS	5%+5%	Increased strength, decreased porosity.
Zhang et al. [66]	FA–MS and FA-MK	10–20%	Compressive strength increased by 18%, flexural strength increased by up to 22%. Modified concretes are characterized by a finer pore network and a denser transition zone.
Huang et al. [67]	FA + Slag	Up to 45%	Concrete's resistance to corrosion by SO_2 and CO_2 increases.
Xiao et al. [68]	FA + MS	Up to 40%	Improved frost resistance and salt corrosion resistance.
Vennapusa et al. [69]	MS	10%	Increased strength properties, decreased porosity.
Janowska-Renkas et al. [70]	Ash / MK	20%/ 15%	High-temperature resistance of hemp concrete increased. Compressive strength increased by over 20%.
Begentayev et al. [71]	MS / MK	15%/10%	Frost resistance increased by 100 cycles, water absorption decreased by 30-35%, and shrinkage strain decreased.
Tlegenov et al. [72]	FA	15%	Thermal conductivity of the composite decreased by 51.47%.
Kumar et al. [73]	MS + Sugarcane ash	Up to 15%	Improved performance characteristics.
Alaj et al. [74]	FA	30%	Saving cement and improving the strength properties of high-strength concrete

As can be seen from the research results of other authors, the optimal ranges for modifying concrete with mineral additives such as MS, FA, waste incineration ash, and ground granulated blast furnace slag, and their combinations, vary from 5% to 45% inclusive, which is also confirmed by several other studies [75-77]. For this study, the optimal content of the complex mineral modifying additive based on man-made waste, introduced in place of part of the cement, does not exceed 20%. Experimental results clearly demonstrate that the use of CMMA significantly improves both the mechanical and durability properties of variatropic concrete. The extent of this improvement depends on both the CMMA content and the production technology used. The 12% optimal CMMA ratio for all production methods implies that concrete performance is dictated by the equilibrium between favorable physicochemical influences and the dilution of cement. The decrease in strength observed above the optimal CMMA ratio (particularly at the 20% level) can be explained by the cement dilution effect. At high admixture rates, the reduction in cement content limits the formation of primary hydration products and leads to an insufficient binder phase. This situation results in a decline in mechanical performance, even if pozzolanic reactions continue. This trend has also been reported similarly in the literature.

Concrete with a variatropic structure and enhanced performance can be produced by CMMA modification, using V, C, and VC technologies. One of the key findings of this study is that concrete produced using the centrifuge (C) and vibro-centrifuge (VC) methods exhibits superior performance compared with the traditional vibration (V) method. This can be explained by the different compaction mechanisms. Under centrifugal force, particles redistribute radially, leading to the formation of a denser structure and a reduction in entrapped air. In the vibro-centrifugal method, the addition of vibration increases particle mobility, reduces segregation, and ensures a more homogeneous distribution of CMMA particles within the matrix. For this reason, VC concretes exhibit the highest mechanical performance and durability. This finding demonstrates that concrete performance is determined not only by material composition but also by interactions with production technology. CMMA is a promising, environmentally friendly additive for concrete production. Importantly, this work proposes a method for producing CMMA as a finished product, ready for sale and use, without any additional preparatory steps. The primary raw material for CMMA production is fly ash, a waste product from solid fuel combustion in thermal power plants. From a logistical and spatial perspective, industrial CMMA production is most efficiently located in a fly ash waste accumulation zone. The industrial CMMA production process is simple and includes the following key process steps: cleaning; drying; dosing; mixing; unloading and packaging.

Using a complex mineral modifying additive based on fly ash waste in concrete technology as a component replacing part of the binder has several important environmental benefits. First, it solves the problem of fly ash accumulation in ash dumps, which negatively impacts the environment. Second, it reduces the consumption of Portland cement required for concrete production. Cement production is associated with significant greenhouse gas emissions, so its partial replacement with CMMA will reduce the carbon footprint. All this contributes to the sustainable development of the construction industry.

The concretes with CMMA that were vibrated, centrifuged, or vibrocentrifuged during the study have a wide range of applications. Concrete produced using the CMMA vibration technology is applicable to the production of reinforced concrete products such as floor slabs, columns, beams, lintels, wall blocks, and other three-dimensional reinforced concrete elements of various configurations. Centrifugation and vibrocentrifugation technologies are also suitable for the production of ring-section reinforced concrete products such as pipes for underground gravity pipelines, power transmission line poles, and lighting and communication poles.

4. Conclusions

This study aimed to develop a complex mineral modifying additive (CMMA) comprising fly ash, microsilica, and metakaolin and to examine the effects of this additive on performing variatropic concrete produced by different production technologies. In this context, concrete samples with different CMMA ratios were produced by vibration (V), centrifuge (C), and vibro-centrifuge (VC) methods. The compressive strength, water impermeability, and freeze–thaw resistance of the samples were determined experimentally. In addition, the microstructural properties of the developed composites were evaluated by SEM and EDS, and the mechanism of action of the additive in cement-based systems was investigated. The following results can be summarized from this study:

1) A complex mineral modifying additive based on industrial waste was obtained with the following composition: FA – 70%; MS – 20%; MK – 10%; C-3 – 0.3% of the final mass of the mineral component mixture. A step-by-step description of the CMMA manufacturing process is provided.

2) The inclusion of up to 16% CMMA increases compressive strength. V, C, and VC concretes containing 12% CMMA exhibit the highest compressive strength. Compressive strength increased by 10.7%, 15.8%, and 18.7% for V, C, and VC concretes, respectively. CMMA exhibits high pozzolanic activity; when included at the optimal dosage, its particles participate in hydration reactions, bind free calcium hydroxide, and promote the formation of additional CSH and CAH gels, which subsequently increase the strength of the cement matrix.

3) The water resistance of concrete improves with the incorporation of CMMA. Composites containing 12% CMMA demonstrated the highest air-penetration resistance among V, C, and VC concretes. Compared with the control compositions, the air penetration resistance of modified V, C, and VC concretes increased by 35.2%, 54.1%, and 68.4%, respectively. Modified V, C, and VC concretes had water resistance grades of W10, W12, and W14. CMMA particles fill the voids between cement grains, and the stable, low-basicity calcium silicate hydroxides formed through pozzolanic reactions improve the structure of the cement matrix by reducing the number of capillary pores. The modified cement matrix has a denser structure and, consequently, better water permeability.

4) The frost resistance of concrete is improved by the inclusion of CMMA. The lowest losses of compressive strength were observed in the V, C, and VC concrete compositions containing 12% CMMA. Compared to the control samples, the losses in compressive strength for the base samples were minimal, amounting to 5.9%, 4.8%, and 3.7%, respectively. Concretes modified with V, C, and VC exhibited frost-resistance grades of F200 and F300. The pozzolanic and microfilling effects of CMMA inclusion leads to a reduction in the volume of capillary pores and, consequently, a decrease in the permeability of the cement matrix. Modifying additive particles form additional closed pores, which reduce the pore fluid pressure in the cement matrix during alternating freeze-thaw cycles.

5) The microstructure of the cement matrices of V, C, and VC concretes modified with a complex mineral modifying additive exhibits some differences. The modified concretes have an organized, dense structure with a cluster of C-S-H and C-A-H zones. The Ca/Si ratios for V, C, and VC concretes are 1.3, 1.1, and 1.2, respectively, directly indicating the presence of low-basic calcium silicate hydroxides C-S-H(I)formed by CMMA modification.

6) Eco-friendly variatropic composites with improved performance have been obtained for use in the manufacture of reinforced concrete products and structures for various purposes.

Although this study is limited to determining the fundamental properties of variatropic concretes containing CMMA, it enables a more precise definition of the application areas of the resulting composites. Future plans include producing a pilot batch of reinforced concrete products using centrifugation and vibrocentrifugation technologies and employing concrete mixes with a complex mineral-modifying additive derived from industrial waste.

5. Declarations

5.1. Author Contributions

Conceptualization, A.N.B., S.A.S., E.M.S., D.M.S., V.V., A.E., and A.C.; methodology, S.A.S., E.M.S, A.N.B., and V.V.; software, A.E. and A.C.; validation, S.A.S., E.M.S., Y.O.Ö., L.R.M., and D.M.S.; formal analysis, A.E., V.V., and A.C.; investigation, A.E. V.V., L.R.M., S.A.S., E.M.S., A.N.B., A.C., and D.M.S.; resources, A.E., A.C., and D.M.S.; data curation, S.A.S. and E.M.S.; writing—original draft preparation, D.M.S., S.A.S., E.M.S., and A.N.B.; writing—review and editing, D.M.S., S.A.S., E.M.S., and A.N.B.; visualization, V.V., S.A.S., E.M.S., and A.N.B.; supervision, Y.O.Ö., project administration, L.R.M.; funding acquisition, D.M.S. All authors have read and agreed to the published version of the manuscript.

5.2. Data Availability Statement

The data presented in this study are available on request from the corresponding author.

5.3. Funding

The research was supported by the Russian Science Foundation, grant No. 25-79-32007, https://rscf.ru/project/25-79-32007/.

5.4. Acknowledgments

The authors would like to acknowledge the administrations of Don State Technical University and Necmettin Erbakan University for their resources and support.

5.5. Conflicts of Interest

The authors declare no conflict of interest.

6. References

[1] da Silva, S. R., & Andrade, J. J. de O. (2022). A Review on the Effect of Mechanical Properties and Durability of Concrete with Construction and Demolition Waste (CDW) and Fly Ash in the Production of New Cement Concrete. Sustainability (Switzerland), 14(11), 6740. doi:10.3390/su14116740.

[2] Abbasnejad, B., Soltani, S., Ahankoob, A., Kaewunruen, S., & Vahabi, A. (2025). Industry 4.0 Technologies for Sustainable Transportation Projects: Applications, Trends, and Future Research Directions in Construction. Infrastructures, 10(5), 104. doi:10.3390/infrastructures10050104.

[3] Dagou, H. H., Gurgun, A. P., Koc, K., & Budayan, C. (2025). The Future of Construction: Integrating Innovative Technologies for Smarter Project Management. Sustainability (Switzerland), 17(10), 4537. doi:10.3390/su17104537.

[4] Niyazbekova, R., Mukhambetov, G., Tlegenov, R., Aldabergenova, S., Shansharova, L., Mikhalchenko, V., & Bembenek, M. (2023). The Influence of Addition of Fly Ash from Astana Heat and Power Plants on the Properties of the Polystyrene Concrete. Energies, 16(10), 4092. doi:10.3390/en16104092.

[5] Li, G., Zhou, C., Ahmad, W., Usanova, K. I., Karelina, M., Mohamed, A. M., & Khallaf, R. (2022). Fly Ash Application as Supplementary Cementitious Material: A Review. Materials, 15(7), 2664. doi:10.3390/ma15072664.

[6] Kang, M., Jia, Y., Guo, P., Ju, Y., & Zhang, H. (2024). Influence of Fly Ash Content on Macroscopic Properties and Microstructure of High-Performance Concrete. Buildings, 14(12), 3844. doi:10.3390/buildings14123844.

[7] Yusuf, M. O., Al-Sodani, K. A. A., Adewumi, A. A., Abdulkareem, M., & Alateah, A. H. (2025). Strength and Microstructural Characteristics of Fly Ash–Waste Glass Powder Ternary Blended Concrete. Materials, 18(19), 4483. doi:10.3390/ma18194483.

[8] Moreira, O., Camões, A., Malheiro, R., & Ribeiro, M. (2025). High-Volume Glass Powder Concrete as an Alternative to High-Volume Fly Ash Concrete. Sustainability (Switzerland), 17(9), 4142. doi:10.3390/su17094142.

[9] Chen, Z., Li, M., & Guan, L. (2024). Safety and Effect of Fly Ash Content on Mechanical Properties and Microstructure of Green Low-Carbon Concrete. Applied Sciences (Switzerland), 14(7), 2796. doi:10.3390/app14072796.

[10] Tseng, K. C., Chi, M., Yeih, W., & Huang, R. (2025). Influence of Slag/Fly Ash as Partial Cement Replacement on Printability and Mechanical Properties of 3D-Printed Concrete. Applied Sciences (Switzerland), 15(7), 3933. doi:10.3390/app15073933.

[11] Peng, Y., Chaimoon, N., Wu, Y., Chen, Y., & Chaimoon, K. (2026). Mechanical Performance, Durability, and Environmental Assessment of Low-Carbon Fiber-Reinforced Reactive Powder Concrete with a High Content of Fly Ash. Infrastructures, 11(3), 91. doi:10.3390/infrastructures11030091.

[12] Liu, F., He, Y., Liu, J., Zhang, F., Hao, X., & Liu, C. (2025). Performance Research of Ultra-High Performance Concrete Incorporating Municipal Solid Waste Incineration Fly Ash. Materials, 18(19), 4623. doi:10.3390/ma18194623.

[13] Abushanab, A., & Vimonsatit, V. (2025). Cost-Effectiveness of Reinforced Recycled Aggregate Concrete Structures with Fly Ash and Basalt Fibres Under Corrosion: A Life Cycle Cost Analysis. Buildings, 15(7), 1167. doi:10.3390/buildings15071167.

[14] Abu Taqa, A., Ebead, U. A., Mohsen, M. O., Aburumman, M. O., Senouci, A., Maherzi, W., & Qtiashat, D. (2025). Experimental Assessment of the Strength and Microstructural Properties of Fly Ash-Containing Basalt Fiber-Reinforced Self-Compacting Sustainable Concrete. Journal of Composites Science, 9(2), 79. doi:10.3390/jcs9020079.

[15] Wang, D., Xu, Z., Yu, Y., Xu, N., Li, C., Tian, X., Wang, H., Shi, F., & Xia, K. (2025). Influence of Carbonized Garbage Fly Ash on the Performance of Foam Concrete. Coatings, 15(7), 736. doi:10.3390/coatings15070736.

[16] Abdoli, M., Mostofinejad, D., Karimi, A., Saljoughian, A., & Eftekhar, M. (2026). Lightweight concrete with improved thermomechanical properties incorporating PCM-infused microsilica additives. Case Studies in Thermal Engineering, 107837. doi:10.1016/j.csite.2026.107837.

[17] Bilal, H., Gao, X., Cavaleri, L., Khan, A., & Ren, M. (2024). Mechanical, Durability, and Microstructure Characterization of Pervious Concrete Incorporating Polypropylene Fibers and Fly Ash/Silica Fume. Journal of Composites Science, 8(11), 456. doi:10.3390/jcs8110456.

[18] Szcześniak, A., Siwiński, J., Stolarski, A., Piekarczuk, A., & Nasiłowska, B. (2025). The Influence of the Addition of Microsilica and Fly Ash on the Properties of Ultra-High-Performance Concretes. Materials, 18(1), 28. doi:10.3390/ma18010028.

[19] Hosseinzadehfard, E., & Mobaraki, B. (2025). Corrosion performance and strain behavior of reinforced concrete: Effect of natural pozzolan as partial substitute for microsilica in concrete mixtures. Structures, 79, 109397. doi:10.1016/j.istruc.2025.109397.

[20] Mazilu, C., Deju, R., Georgescu, D. P., Apostu, A., & Barbu, A. (2024). Effects of Micro- and Nanosilica on the Mechanical and Microstructural Characteristics of Some Special Mortars Made with Recycled Concrete Aggregates. Materials, 17(12), 2791. doi:10.3390/ma17122791.

[21] Rajagopal, M. R., Ganta, J., & Pamu, Y. (2024). Enhancing the Strength and the Environmental Performance of Concrete with Pre-Treated Crumb Rubber and Micro-Silica. Recycling, 9(3), 32. doi:10.3390/recycling9030032.

[22] Rogojsz, G., & Rudnicki, T. (2025). The Influence of Mineral Additives on Aggregate Reactivity. Materials, 18(1), 7. doi:10.3390/ma18010007.

[23] Amer Salih, M., Kamil Ahmed, S., & Salih Mohammed, A. (2025). Performance of Sustainable Underwater Concrete Containing GGBS and Micro Silica with Anti-Washout. Civil Engineering Journal, 11(12), 5238–5255. doi:10.28991/cej-2025-011-12-018.

[24] Zhagifarov, A. M., Akhmetov, D. A., Suleyev, D. K., Zhumadilova, Z. O., Begentayev, M. M., & Pukharenko, Y. V. (2024). Investigation of Hydrophysical Properties and Corrosion Resistance of Modified Self-Compacting Concretes. Materials, 17(11), 2605. doi:10.3390/ma17112605.

[25] Beskopylny, A. N., Stel'makh, S. A., Shcherban', E. M., Shakhalieva, D. M., Chernil'nik, A., Shcherban', N., Vyalikov, I., & Budovskiy, A. (2026). Mechanical Properties and Microstructure of Environmentally Friendly Foam Concrete with Fly Ash Modified with Micro- and Nano-SiO2. Materials, 19(4), 814. doi:10.3390/ma19040814.

[26] Khan, S., parveez, M., & Tantray, M. A. (2025). Metakaolin-infused concrete for sustainable and durable building rehabilitation. Journal of Building Pathology and Rehabilitation, 10(1), 66. doi:10.1007/s41024-025-00578-9.

[27] Bede Odorčić, N., & Kravanja, G. (2022). Combined Effects of Metakaolin and Hybrid Fibers on Self-Compacting Concrete. Materials, 15(16), 5588. doi:10.3390/ma15165588.

[28] Rose, D., & Shirzad, S. (2024). Innovations in Green Concrete: Combining Metakaolin and Arundo Grass Biochar for Enhanced Sustainability. Sustainability (Switzerland), 16(24), 11219. doi:10.3390/su162411219.

[29] Li, T., Chen, X., Yang, W., Zhan, M., Hao, L., Zhang, L., & Yang, Y. (2025). Study on Carbonization Performance of Metakaolin on Tailings- and Recycled-Concrete-Based Green Concrete. Buildings, 15(13), 2262. doi:10.3390/buildings15132262.

[30] Imoh, U. U., Habashneh, M., Kaine, S. C., Babafemi, A. J., Hassan, R., & Movahedi Rad, M. (2025). Metakaolin-Enhanced Laterite Rock Aggregate Concrete: Strength Optimization and Sustainable Cement Replacement. Buildings, 15(24), 4553. doi:10.3390/buildings15244553.

[31] Malaiškienė, J., Škamat, J., Kizinievič, O., & Girskas, G. (2025). Synergistic Effect of Metakaolin Waste and Nano-Silica on the Properties of Ultra-High-Performance Concrete. Processes, 13(11), 3614. doi:10.3390/pr13113614.

[32] Jahami, A., Frangieh, H., Assaad, J., Alkhatib, A., Avci-Karatas, C., & Chieffo, N. (2025). Experimental and Numerical Study Assessing the Synergistic Effect of Metakaolin and Waste Glass on the Concrete Mechanical and Structural Properties. Buildings, 15(17), 3185. doi:10.3390/buildings15173185.

[33] Wang, M., Zhang, X., Zhang, B., Zhang, D., Wang, D., & Zhang, Y. (2025). Model Experimental Investigation on the Mechanical Properties of Recycled Aggregate Concrete Curbs by Incorporating Metakaolin and Basalt Fibre. Buildings, 15(17), 3059. doi:10.3390/buildings15173059.

[34] Dziedzic, K., Brachaczek, A., Nowicki, D., & Glinicki, M. A. (2025). Mitigation of Alkali–Silica Reactivity of Greywacke Aggregate in Concrete for Sustainable Pavements. Sustainability (Switzerland), 17(15), 6825. doi:10.3390/su17156825.

[35] Elbialy, S., El-Latief, A. A., Al-Jabali, H. M., Elsayed, H. A., & Shawky, S. M. M. (2024). Enhancing the Properties of Steel Fiber Self-Compacting NaOH-Based Geopolymer Concrete with the Addition of Metakaolin. Civil Engineering Journal (Iran), 10(7), 2244–2260. doi:10.28991/CEJ-2024-010-07-011.

[36] Rashid, K., Farooq, S., Mahmood, A., Iftikhar, S., & Ahmad, A. (2020). Moving towards resource conservation by automated prioritization of concrete mix design. Construction and Building Materials, 236, 117586. doi:10.1016/j.conbuildmat.2019.117586.

[37] Gowram, I., M, B., Sudhir, M. R., Mohan, M. K., & Jain, D. (2021). Efficacy of natural zeolite and metakaolin as partial alternatives to cement in fresh and hardened high strength concrete. Advances in Materials Science and Engineering, 2021(1), 4090389. doi:10.1155/2021/4090389.

[38] Vallières, P. L., Graveline, C., Daoust, K., d'Espinose de Lacaillerie, J. B., Tagnit-Hamou, A., & Claverie, J. P. (2026). Increasing the metakaolin content of blended cements by cationic latex adsorption: Towards more sustainable concrete. Cement and Concrete Research, 204, 108190. doi:10.1016/j.cemconres.2026.108190.

[39] Valizadeh Kiamahalleh, M., Gholampour, A., Rezaei Shahmirzadi, M., Ngo, T. D., & Ozbakkaloglu, T. (2024). Mechanical, Durability, and Microstructure Assessment of Wastepaper Fiber-Reinforced Concrete Containing Metakaolin. Materials, 17(11), 2608. doi:10.3390/ma17112608.

[40] Owaid, A. M., Jabbar, N. F., Owaid, H. M., & Al-Abbas, B. H. (2026). Comprehensive mechanical, durability, and microstructural assessment of lightweight GGBS–metakaolin geopolymer concrete incorporating LECA. Construction and Building Materials, 506, 144961. doi:10.1016/j.conbuildmat.2025.144961.

[41] Majhi, B., Pradhan, S., Sultana, B., & Tudu, C. (2025). An empirical study examining the characteristics of metakaolin-based concrete with recycled waste concrete coarse aggregate. Innovative Infrastructure Solutions, 10(9), 443. doi:10.1007/s41062-025-02248-8.

[42] Abdelmelek, N., S. Alimrani, N., Krelias, N., & Lubloy, E. (2021). Effect of Elevated Temperatures on Microstructure of High Strength Concrete Based-Metakaolin. Journal of King Saud University - Engineering Sciences, 38, 25. doi:10.1016/j.jksues.2021.08.001.

[43] Kumar, K. M., Subramanian, S. N. S., & Sekar, A. (2025). Effect of fly ash cenosphere concrete under elevated temperature. Environmental Science and Pollution Research, 32, 31725–31742. doi:10.1007/s11356-025-36898-z.

[44] Chahar, A. S., & Pal, P. (2024). Investigation on Binary, Ternary, and Quaternary Blended Cement Mortar Integrated with Mineral Additives. Iranian Journal of Science and Technology - Transactions of Civil Engineering, 48(5), 3407–3439. doi:10.1007/s40996-024-01384-y.

[45] Wang, C., Zhao, X., Fu, S., Zhao, Y., Wang, Y., & Zhao, J. (2025). Effect of Industrial Waste Slurry Coating on the Performance of Recycled Concrete Made with Waste Incineration Bottom Ash. Journal Wuhan University of Technology, Materials Science Edition, 40(4), 1067–1077. doi:10.1007/s11595-025-3145-1.

[46] Compaore, A., Toure, J. Y. N. Z. K., Klenam, D. E. P., Merenga, A. S., Asumadu, T. K., Obayemi, J. D., Rahbar, N., Migwi, C., & Soboyejo, W. O. (2025). Foam concrete with mineral additives: from microstructure to mechanical/physical properties, workability and durability. Open Ceramics, 23, 100812. doi:10.1016/j.oceram.2025.100812.

[47] Hou, S., Guo, Y., Sun, J., Jiang, J., Gao, H., & Liu, J. (2025). Prospect of gold tailings as a new mineral admixture: Effect on hydration, pore structure and mechanical properties of concrete. Materials Today Sustainability, 29, 101078. doi:10.1016/j.mtsust.2025.101078.

[48] Risdanareni, P., Dewi, V. A. K., Wahyuono, R. A., Ekaputri, J. J., Olivia, M., Farnam, Y., & De Belie, N. (2025). Potential use of fly ash based nano silica as mineral additive to improve the mechanical properties of self-healing mortar. Case Studies in Construction Materials, 23, 5611. doi:10.1016/j.cscm.2025.e05611.

[49] Shcherban', E. M., Stel'makh, S. A., Beskopylny, A. N., Mailyan, L. R., Shakhalieva, D. M., Chernil'nik, A., Matua, V. P., & Nikolenko, D. A. (2026). Study of TiO2 and Al2O3 Nanoparticles' Influence on the Variatropic Concrete Properties. Materials, 19(6), 1081. doi:10.3390/ma19061081.

[50] Kliukas, R., Lukoševičiene, O., Jaras, A., & Jonaitis, B. (2020). The mechanical properties of centrifuged concrete in reinforced concrete structures. Applied Sciences (Switzerland), 10(10), 3570. doi:10.3390/app10103570.

[51] Shcherban', E. M., Stel'makh, S. A., Mailyan, L. R., Beskopylny, A. N., Mailyan, A. L., Shcherban', N., Chernil'nik, A., & Elshaeva, D. (2025). Composition and Properties of Lightweight Concrete of Variotropic Structure Based on Combined Aggregate and Microsilica. Buildings, 15(3), 346. doi:10.3390/buildings15030346.

[52] Beskopylny, A. N., Shcherban, E. M., Stel'makh, S. A., Mailyan, L. R., Meskhi, B., Chernil'nik, A., & El'shaeva, D. (2023). Influence of Variatropy on the Evaluation of Strength Properties and Structure Formation of Concrete under Freeze-Thaw Cycles. Journal of Composites Science, 7(2), 58. doi:10.3390/jcs7020058.

[53] EN 12390-1:2021. (2021). Testing Hardened Concrete – Part 1: Shape, Dimensions and Other Requirements of Specimens and Moulds. European Committee for Standardization (CEN), Brussels, Belgium.

[54] EN 12390-2:2019. (2019). Testing hardened concrete - Part 2: Making and curing specimens for strength tests. European Committee for Standardization (CEN), Brussels, Belgium.

[55] EN 12390-3:2019. (2019). Testing hardened concrete - Part 3: Compressive strength of test specimens. European Committee for Standardization (CEN), Brussels, Belgium.

[56] EN 12390-4:2019. (2019). Testing hardened concrete - Compressive strength. Specification for testing machines. European Committee for Standardization (CEN), Brussels, Belgium.

[57] GOST 12730.5-2018. (2019). Concretes. Methods for determination of water tightness. Standartinform, Moscow, Russia.

[58] GGOST 10060-2012 (2014). Concretes. Concretes. Methods for determination of frost-resistance. Standartinform, Moscow, Russia.

[59] Anjos, M. A. S. do., Camões, A., Malheiro, R., Maia Pederneiras, C., & Peixoto, L. K. S. (2025). Experimental Study of Carbonation and Chloride Resistance of Self-Compacting Concretes with a High Content of Fly Ash and Metakaolin, with and Without Hydrated Lime. Materials, 18(2), 422. doi:10.3390/ma18020422.

[60] Degani, I. M., Maddalena, R., & Kulasegaram, S. (2026). Influence of Varying Curing Temperatures on the Mechanical and Durability-Related Performance of Multi-SCM Blended High-Strength Self-Compacting Concrete. Buildings, 16(5), 910. doi:10.3390/buildings16050910.

[61] Hayek, M., El Bitouri, Y., & Yahia, A. (2025). Time-Dependent Structuration of Cement Pastes with Mineral Additions: A Yield Stress-Based Approach. Buildings, 15(23), 4297. doi:10.3390/buildings15234297.

[62] Ali, T., Qureshi, M. Z., Inam, I., Kahla, N. Ben, Ahmed, H., Ajwad, A., & Adnan, M. (2025). Sustainable concrete production through the integration of waste foundry sand, fly ash, silica fume and metakaolin. Scientific Reports, 15(1), 27512. doi:10.1038/s41598-025-13277-9.

[63] Malaiškienė, J., & Jakubovskis, R. (2025). Influence of Pozzolanic Additives on the Structure and Properties of Ultra-High-Performance Concrete. Materials, 18(6), 1304. doi:10.3390/ma18061304.

[64] Puzatova, A. V., Dmitrieva, M. A., Tovpinets, A. O., & Leitsin, V. V. (2024). Study of Structural Defects Evolution in Fine-Grained Concrete Using Computed Tomography Methods. Advanced Engineering Research (Rostov-on-Don), 24(3), 227–237. doi:10.23947/2687-1653-2024-24-3-227-237.

[65] Nesvetaev, G. V., Koryanova, Y. I., & Shut, V. V. (2025). Autogenous Shrinkage of Concretes from Highly Mobile and Self-Compacting Mixtures. Modern Trends in Construction, Urban and Territorial Planning, 4(1), 41–53. doi:10.23947/2949-1835-2025-4-1-41-53.

[66] Zhang, J., Saleh, M. A., Abdelgader, H. S., Murali, G., Zar, A., & Alnagasa, A. A. (2026). Development of sustainable low carbon preplaced aggregate concrete with Portland limestone cement, Metakaolin, silica fume and fly ash: Evaluating binary and ternary binder systems for strength and microstructural properties. Results in Engineering, 29, 109679. doi:10.1016/j.rineng.2026.109679.

[67] Huang, J., Niu, D., Lv, Y., Wu, H., & Li, Z. (2025). Investigation of mineral admixtures on the resistance of concrete exposed to industrial SO2 and CO2 corrosion. Journal of Building Engineering, 107, 112749. doi:10.1016/j.jobe.2025.112749.

[68] Xiao, X., Xie, Y., Hao, T., Jiang, C., Yuan, J., & Xiao, F. (2025). Salt-frost resistance mechanisms and improvement of surface concrete with mineral admixtures in two-lift airport pavement. Construction and Building Materials, 484, 141882. doi:10.1016/j.conbuildmat.2025.141882.

[69] Vennapusa, C. S. R., & Eluru, A. (2025). Experimental study on (OPC concrete), inclusive of using plastic bottle flakes with mineral and chemical admixtures for environmental sustainability. Progress in Engineering Science, 2(3), 100128. doi:10.1016/j.pes.2025.100128.

[70] Janowska-Renkas, E., Król, A., Klementowski, I., & Sokolski, M. (2025). Hemp Concrete with Mineral Additives as a Durable and Fire-Resistant Material in Green Construction. Materials, 18(9). doi:10.3390/ma18091905.

[71] Begentayev, M. M., Kuldeyev, E. I., Akhmetov, D. A., Zhumadilova, Z. O., Suleyev, D. K., Utepov, Y. B., Awwad, T., & Kuttybay, M. T. (2025). The Effect of Mineral Fillers on the Rheological and Performance Properties of Self-Compacting Concretes in the Production of Reinforced Concrete Products. Journal of Composites Science, 9(5), 235. doi:10.3390/jcs9050235.

[72] Tlegenov, R. B., Niyazbekova, R. K., Jexembayeva, A. E., Korniejenko, K., Aruova, L. B., Aldabergenova, S. S., & Maykonov, A. S. (2024). The Effect of Fly Ash Additive on the Thermal Conductivity of Polystyrene Concrete. Buildings, 14(9), 2850. doi:10.3390/buildings14092850.

[73] Kumar, A., Kumar, R., Bheel, N., Ali, S., Shaikh, F. A., Yousfani, A. M., & Rizvi, S. H. (2025). Effect of local metakaolin and waste sugarcane bagasse ash on mechanical properties and embodied carbon of sustainable concrete. Innovative Infrastructure Solutions, 10(4), 127. doi:10.1007/s41062-025-01945-8.

[74] Alaj, A., Krelani, V., & Numao, T. (2023). Effect of Class F Fly Ash on Strength Properties of Concrete. Civil Engineering Journal (Iran), 9(9), 2249–2258. doi:10.28991/CEJ-2023-09-09-011.

[75] Dvorkin, L., Bordiuzhenko, O., Mierzwiński, D., Tracz, T., & Sitarz, M. (2024). Water Impermeability of Self-Compacting Fly-Ash-Containing Concrete. Applied Sciences (Switzerland), 14(13), 5373. doi:10.3390/app14135373.

[76] Chen, Z., Liu, M., Zhang, Y., & Jia, S. (2026). Prediction of the Time-Dependent Elastic Modulus of Fly-Ash Concrete under Sustained Loads. Materials, 19(3), 559. doi:10.3390/ma19030559.

[77] Kulikov, B. P., Tarasov, I. V., Bezrukikh, A. I., Konstantinov, I. L., & Voroshilov, D. S. (2025). Investigation properties of microsilica to assess the possibility of its use as an additive in concrete production. Construction Materials and Products, 8(3), 5. doi:10.58224/2618-7183-2025-8-3-5.